Article

TEFDDOLs (alpha,alpha,alpha',alpha'-Tetrakisperfluoroaryl/alkyl-2,2'-dimethyl-1,3-dioxolan-4,5-dimethanols): Highly Fluorinated Chiral H-Bond Donors and Bronsted-Acids with Distinct H-Bonding Patterns and Supramolecular Achitectures.

Albrecht Berkessel, Sonja S. Vormittag, Nils E. Schlörer, and Jörg-M. Neudörfl

J. Org. Chem., **Just Accepted Manuscript** • Publication Date (Web): 02 Oct 2012

TEFDDOLs (α,α,α',α'-Tetrakisperfluoroaryl/alkyl-2,2'-dimethyl-1,3-dioxolan-4,5-dimethanols): Highly Fluorinated Chiral H-Bond Donors and Brønsted-Acids with Distinct H-Bonding Patterns and Supramolecular Achitectures.

Albrecht Berkessel,* Sonja S. Vormittag, Nils E. Schlörer, and Jörg-M. Neudörfl

[†]Department of Chemistry (Organic Chemistry), University of Cologne, Greinstr. 4, 50939 Cologne, Germany; Fax: (+49) 221-4705102

*E-mail: berkessel@uni-koeln.de

Table of Contents Graphic

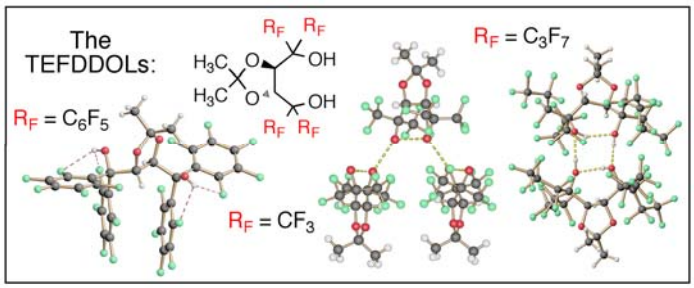

Abstract

The synthesis of six enantiopure α,α,α',α'-tetrakisperfluoroalkyl/aryl-2,2'-dimethyl-1-3-dioxolan-4,5-dimethanols (TEFDDOLs), by addition of perfluorinated organolithium reagents or Ruppert's reagent (TMS-CF_3) to *iso*-propylidene tartaric dichloride, is reported. X-Ray crystal structures of the TEFDDOLs alone or in complexes with H-bond acceptors such as

water or DABCO revealed that this new class of highly fluorinated chiral 1,4-diols forms distinct intra- and intermolecular H-bond patterns. Intramolecular OH-OH bonding accounts for the relatively high acidity of the perfluoroalkyl TEFDDOLs [pK_a in DMSO: tetrakis-CF_3: 5.7; tetrakis-C_2F_5: 2.4]. For the tetrakis-perfluorophenyl TEFDDOL, a quite unusual "pseudo-anti" conformation of the diol, with no intramolecular (and no intermolecular) OH-OH bonds was found both in the crystal and in solution (DOSY- and NOESY-NMR). The latter conformation results from a total of four intramolecular OH-F_{aryl} hydrogen bonds overriding OH-OH bonding. Due to their H-bonding properties, the TEFDDOLs are promising new building blocks for supramolecular and potentially catalytic applications.

---

1. Introduction

Over recent years, selective hydrogen bonding has been recognized as one of the most important principles in (asymmetric) organocatalysis.[1] The most broadly applicable hydrogen bond donor motifs are (thio)ureas **1**,[2] more recently squareamides **2**,[3] and TADDOLs[4] **3** (Figure 1). Whereas (thio)ureas and squaramides are typically able to donate two H-bonds to

Figure 1. Typical H-bond donor patterns of (thio)ureas **1**, squaramides **2** and TADDOLs **3**. TADDOL: α,α,α',α'-tetraaryl-2,2-dimethyl-1,3-dioxolane-4,5-dimethanol; **A**: H-bond acceptor.

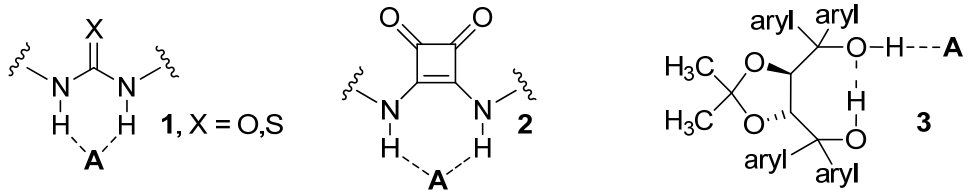

a suitable acceptor, TADDOLs - with only few exceptions - typically form one intramolecular and one intermolecular hydrogen bond.[5] As a consequence, the intermolecular H-bond donor

ability of TADDOLs is enhanced, a situation resembling Yamamoto's concept of "Brønsted acid assisted Brønsted acids" (BBAs).[6]

On the other hand, fluorinated alcohols such as 1,1,1,3,3,3-hexafluoro-2-propanol ("hexafluoro-*iso*-propanol", HFIP, **4**, Figure 2) have served in numerous instances as solvents with remarkable properties.[7] For example, their high solvation power, together with low nucleophilicity, allowed the generation and observation of reactive cationic or radical-cationic species.[8] Additionally, fluorination accounts for their increased acidity, relative to non-fluorinated analogs.[7] Not surprisingly, they are good H-bond donors and poor acceptors. Fluorinated alcohols as solvents furthermore promote the epoxidation of olefins and the sulfoxidation of thioethers.[9] A recent study of ours established accelerations (of epoxidation) up to 100.000-fold, relative to conventional solvents such as 1,4-dioxane.[10]

Altogether, we settled on compound **5a** (Figure 2) as a fluoroalcohol (here: HFIP)–TADDOL hybrid. In analogy to the TADDOLs, we dubbed the α,α,α',α'-tetrakis(perfluoroalkyl/aryl)-2,2-dimethyl-1,3-dioxolane-4,5-dimethanols **5** "TEFDDOLs". In this article, we describe (i) the synthesis of the hitherto unknown tetrakis-perfluoroalkyl-TEFDDOLs [CF_3 (**5a**), C_2F_5 (**5b**), *n*-C_3F_7 (**5c**), *n*-C_4F_9 (**5d**), *n*-C_6F_{13} (**5e**); Figure 2], (ii) a largely improved synthesis of the tetrakis-pentafluorphenyl-TEFDDOL **5f**, (iii) X-ray crystal structures of all TEFDDOLs made, and of H-bonded aggregates thereof with H-bond acceptors such as water and amines, and (iv) NMR studies (DOSY) showing that the dimerization of TEFDDOLs by H-bonding (as observed in the crystal) persists in solution. It is furthermore shown by NOESY-NMR that the quite unusual "pseudo-anti" conformation found for **5f** in the crystal persists in solution. pK_a-values for the TEFDDOLs **5a**, **5b** and **5f** have been reported from this laboratory earlier,[11] revealing *inter alia* the remarkably high acidity of the "parent" tetrakis-CF_3-TEFDDOL **5a** [pK_a

(DMSO) = 5.7], and in particular of its C_2F_5- homologue **5b** [pK_a (DMSO) = 2.4]. These data suggest that TEFDDOLs may not only be suitable as hydrogen bond donors, but may just as well have potential as chiral Brønsted acid organocatalysts.[12]

Figure 2. Top: TEFDDOL **5a** as a covalent and chiral analogue of a supramolecular HFIP (**4**) dimer; **A**: H-bond acceptor. Bottom: TEFDDOLs **5a-f** reported in this article.

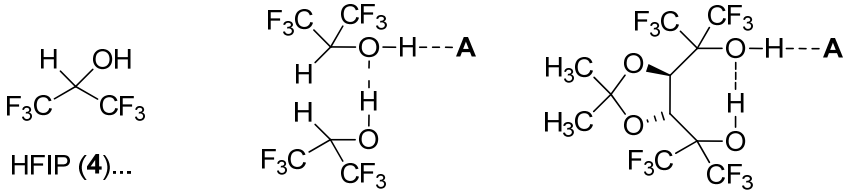

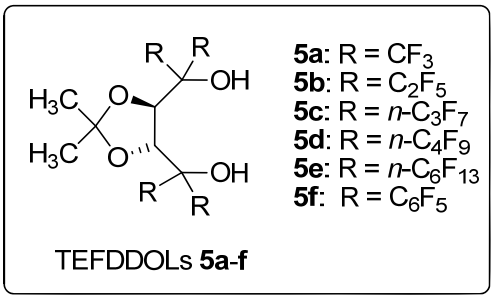

Similar to the synthesis of the TADDOLs **3** by Seebach et al.,[5a] we envisaged the addition of perfluoroalkyl lithium reagents[13] to activated forms (ester, acid chloride) of *iso*-propylidene tartaric acid as the most straightforward approach to the TEFDDOLs **5b-f**. An exception is the tetrakis-trifluoromethyl-TEFDDOL **5a**, as it is known that trifluoromethyl lithium is too unstable to serve as a CF_3-nucleophile.[13] In this particular case, Ruppert's reagent (CF_3-TMS, **6**) was considered as an alternative CF_3-donor.[14] Before our study, the only TEFDDOL known in the literature was the tetrakis-pentafluorophenyl-TADDOL **5f** (Figure 2), reported by Hafner et al.[15] In our hands, however, the procedure by Hafner et al.

(employing tartaric ester) gave at best yields < 10 %. As described in detail below, a quite satisfactory yield of 70 % resulted upon switching to the acid chloride as electrophile and in situ-quenching.[16]

2. Results and Discussion

2.1 Syntheses. For the tartaric acid electrophiles, we found in extensive optimization studies (not reported) that (*R*,*R*)-*iso*-propylidene tartaric acid dichloride **7** invariable gave superior yields of TEFDDOLs compared to e.g. tartaric esters. This starting material **7** was prepared from (*R*,*R*)-*iso*-propylidene tartaric disodium salt according to Klotz et al.[17] Upon sublimation, material suitable for X-ray crystallography was obtained. The X-ray crystal structure of **7** is shown in Figure 3.

Figure 3. X-Ray crystal structure of (*R*,*R*)-*iso*-propylidene tartaric acid dichloride (**7**).

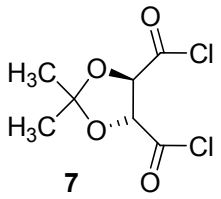

7

2.1.1 Synthesis of the TEFDDOL 5a using Ruppert's reagent (6). When the acid chloride **7** was treated with increasing amounts of Ruppert's reagent **6** and tetramethylammonium fluoride[18] at -50 °C in DME, significant conversion was observed beginning from ca. 4 equiv. of reagent and fluoride used. A trifluoromethylation product **8** was isolated in 33 % yield after aqueous workup which, however, turned out not to be the desired TEFDDOL **5a**. As evidenced by NMR and in particular by X-ray crystallography, the "semi-trifluoromethylated"

tartaric acid **8** was formed under these conditions (Scheme 1, top). To our delight, increasing the amount of TMS-CF_3 (**6**) to ca. 7 equiv. resulted in the formation of the TEFDDOL **5a** which could be isolated in 20 % yield (Scheme 1, bottom).

Scheme 1. Trifluoromethylation of *iso*-propylidene tartaric acid dichloride (**7**), using Ruppert's reagent (**6**).

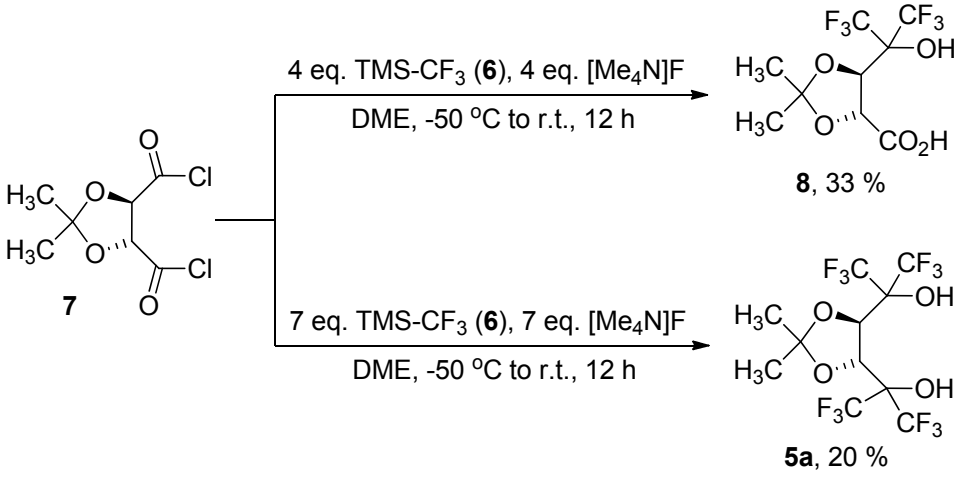

The X-ray crystal structures of the tartaric acid bis-trifluoromethyl derivative **8** and of the tetrakis-trifluoromethyl TEFDDOL **5a** are shown in Figure 4. The water-free crystals needed for the X-ray structural analysis of pure **5a** were obtained by sublimation under vacuum in a sealed tube, and through a layer of 4 Å molecular sieves (see section II.3 below for the structure of the 2:1 complex of **5a** with water).

Figure 4. X-Ray crystal structures of the tartaric acid bis-trifluoromethyl derivative **8** and of the tetrakis-trifluoromethyl TEFDDOL **5a**.

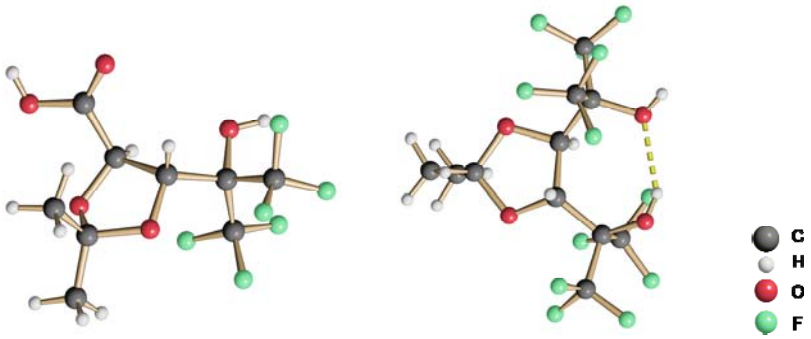

8 **5a**

The crystal packing of the bis-trifluoromethyl carboxylic acid **8** revealed numerous hydrogen bonding interactions (Figure 5) which result in the aggregation of three molecules of **8** to form repeating "triplets". The most prominent interaction is a hydrogen bond between the OH-group of the carboxylic acid and one oxygen atom of the dioxolane ring of a neighboring molecule. A third molecule of **8** is involved in the sense that the hydroxyl group of its fluoroalcohol moiety is hydrogen bonded to the carbonyl oxygen atom of the first molecule (Figure 5).

Figure 5. Crystal packing diagram of the bis-trifluoromethyl carboxylic acid **8**.

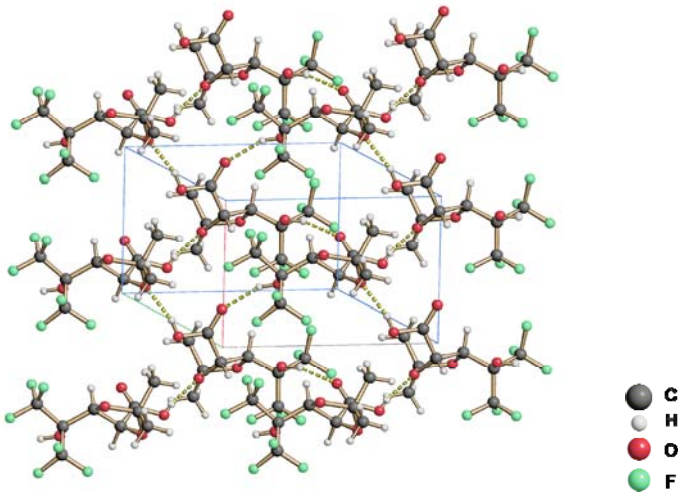

As may have been expected, the preparation of the tetrakis-CF_3-TEFDDOL **5a** was not successful when halogen-lithium exchange on CF_3I was tried for the generation of the CF_3-nucleophile. No trifluoromethylation of *iso*-propylidene tartaric acid dichloride (**7**) could be observed. The latter result is not surprising as it is well known that even at low temperatures, trifluoromethyl lithium or the corresponding Grignard reagent are unstable and decompose instantaneously to difluorocarbene by elimination of the metal fluoride.[13]

2.1.2 Synthesis of the TEFDDOLs 5b-f using perfluorinated organolithium reagents. In our optimized procedure, *iso*-propylidene tartaric acid dichloride (**7**) and the perfluorinated alkyl/aryl iodide or bromide (ca. 7 equiv.) were dissolved together in diethyl ether at -78 °C. Methyl lithium (5 equiv.), stabilized by lithium bromide, was then added in one portion. After 1 h, aqueous work-up followed by chromatographic purification afforded the desired products with yields ranging from 15-70 % (Scheme 2).

Scheme 2. Synthesis of the TEFDDOLs **5b**-**f** starting from *iso*-propylidene tartaric acid dichloride **7**.

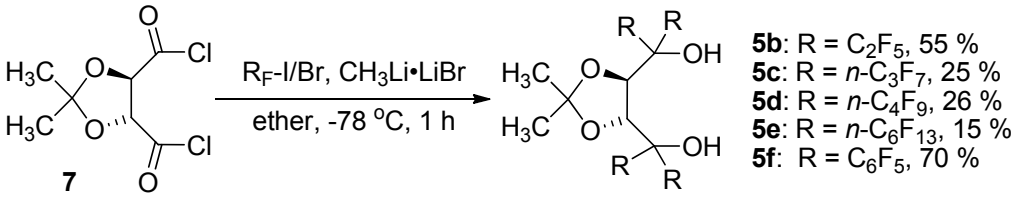

Halogen-lithium exchange is sufficiently fast to be performed in the presence of the electrophile **7** - no side reactions of methyl lithium with tartaric acid dichloride **7** have been observed. With regard to the yields of TEFDDOLs **5b**-**f**, the in situ-quenching method

described above proved superior to the sequential formation of the perfluoroalkyl lithium intermediates, followed by addition of the acid chloride **7**. By the same token, the acid chloride **7** proved superior to other tartaric acid derived electrophiles, such as esters. As summarized in Scheme 2, we sucessfully introduced pentafluorophenyl-, pentafluoroethyl-, heptafluoro-*n*-propyl-, nonafluoro-*n*-butyl- and tridecafluoro-*n*-hexyl-groups using lithium-halogen exchange. As expected, CF_3I did not afford any of the CF_3-TEFDDOL **5a** under the conditions described above. However, as mentioned above (2.1.1), this "parent" TEFDDOL was accessible using Ruppert's reagent (CF_3-TMS, **6**) as the trifluoromethyl source.

2.2 Solid State Structures.

2.2.1 X-Ray crystal structures of the TEFDDOLs 5a-f: intramolecular hydrogen bonding in 5a-e, but not in 5f. All TEFDDOLs **5a**-**f** were characterized by x-ray crystallography. The molecular structures of **5b**-**f** are shown in Figure 6. Note that all perfluoroalkyl TEFDDOLs **5b**-**e** show - just as the parent system **5a** (Figure 4) - the expected intramolecular OH-OH hydrogen bonding. In line with this, the "pseudo-torsion angle" O-$C_{carbinol}$-$C_{carbinol}$-O is low and in the range of ca. 20-30^o. As the sole exception, the tetrakis-pentafluorophenyl TEFDDOL **5f** adopts a completely different conformation in the crystal: There is no intramolecular (and no intermolecular) OH-OH bonding. Instead, each one of the two hydroxyl groups forms a bifurcated hydrogen bond to two "ortho" fluorine atoms on the phenyl rings. A "pseudo-anti" arrangement of the two hydroxyl groups results, with a "pseudo-torsion angle" O-$C_{carbinol}$-$C_{carbinol}$-O of 170.7 (2)^o. The H-F distances are in the range of 2.23 - 2.29 Å. These values coincide very well with the H-F bond length of 2.23 Å observed earlier in intramolecularly H-F bonded 2-fluorophenyldiphenylmethanol.[19]

Figure 6. Crystal structures of TEFDDOLs **5b**-**f**. Disorder of OH H-atoms is not shown. The C_2F_5-groups of **5b** are disordered, and only one orientation is shown.

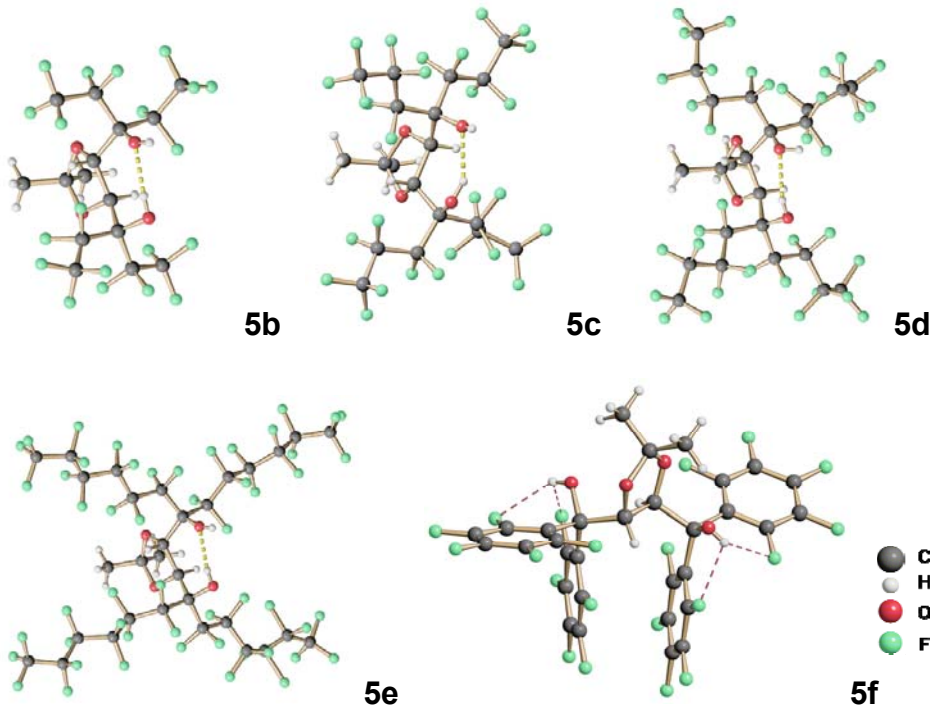

Note that in the area of TADDOLs, of the 161 crystal structures deposited in the CCDC-file, only two show the “pseudo-anti” arrangement of the two hydroxyl groups.[20] In both of these cases, the TADDOL incorporates a diphenyl-dioxolane (i.e. a benzophenone acetal). Thus, **5f** is the only case of a dimethyl-dioxolane (i.e. acetone acetal) showing “pseudo-anti” conformation. In the case of the two TADDOLs, the "pseudo-anti" conformation is enforced by non-bonding interactions involving the acetalic phenyl groups. In other words, steric hindrance overrides the attractive intramolecular OH-OH bonding. In the case of the tetrakis-pentafluorophenyl TEFDDOL **5f,** a total of four intramolecular OH-F bonds override

one OH-OH bond. Note that the "pseudo-anti" conformation of TEFDDOL **5f** persists in solution (see section 2.3 below), thus it is clearly not an effect of crystal packing.

2.2.2 X-Ray crystal structures of the TEFDDOLs 5a-f: modes of intermolecular hydrogen bonding. To our delight, the X-ray crystal structure of the tetrakis-trifluoromethyl TEFDDOL **5a** monomer (Figure 7), which could be obtained in water-free form by sublimation through molecular sieves (4Å), revealed a hydrogen bond network reminiscent of that found for HFIP (**4**) itself.[10] Most importantly, the OH-groups of **5a** form an endless, zig-zag-patterned ribbon. In this endless sequence of intra- and intermolecular hydrogen bonds, the

Figure 7. Layered crystal packing of intra- and intermolecular hydrogen bonded TEFDDOL **5a**.

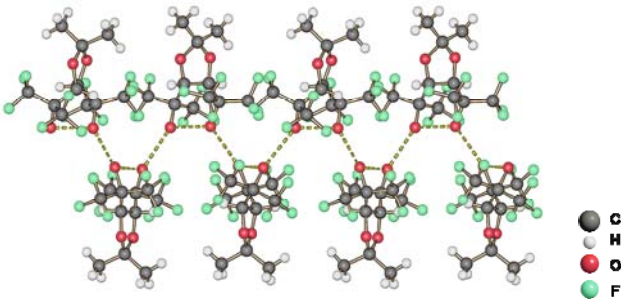

intramolecular O-H-O bonds have an O-O-distance of 2.752 Å (average over the three independent molecules in the unit cell), wheras the intermolecular ones are on the average 3.079 Å in length. Furthermore, it is interesting to note that the crystal shows a "trifle"-type separation of the polar OH-regime, mantled by "fluorous" layers which are made up by the closely interacting CF_3-groups. These fluorous layers are again followed by a medium-

polarity hydrocarbon layer, consisting of the oxygen atoms and the methyl groups of **5a**'s acetal substructure (Figure 7).

The crystal structures of tetrakis-pentafluoroethyl TEFDDOL **5b** and its homologue **5c** revealed a different mode of intermolecular hydrogen bonding interaction. As shown in Figure 8, these TEFDDOLs are characterized by hydrogen bonded dimers. Dimerization is brought about by intermolecular hydrogen O-H-O bonding, typically 2.745 Å in length, in addition to the typical intramolecular O-H-O-bonding (2.695 Å on the average). Most likely, the increasing size of the perfluoroalkyl groups (C_2F_5, and C_3F_7 vs. CF_3) prohibits the formation

Figure 8. Cyclic hydrogen bond networks observed for the tetrakis-pentafluoroethyl (**5b**), the tetrakis-heptafluoro-*n*-propyl-TEFDDOL (**5c**), the tetrakis-nonafluoro-*n*-butyl (**5d**), and the tetrakis-tridekafluoro-*n*-hexyl-TEFDDOL (**5e**). Disorder of OH H-atoms is not shown. The C_2F_5-groups of **5b** are disordered, and only one orientation is shown.

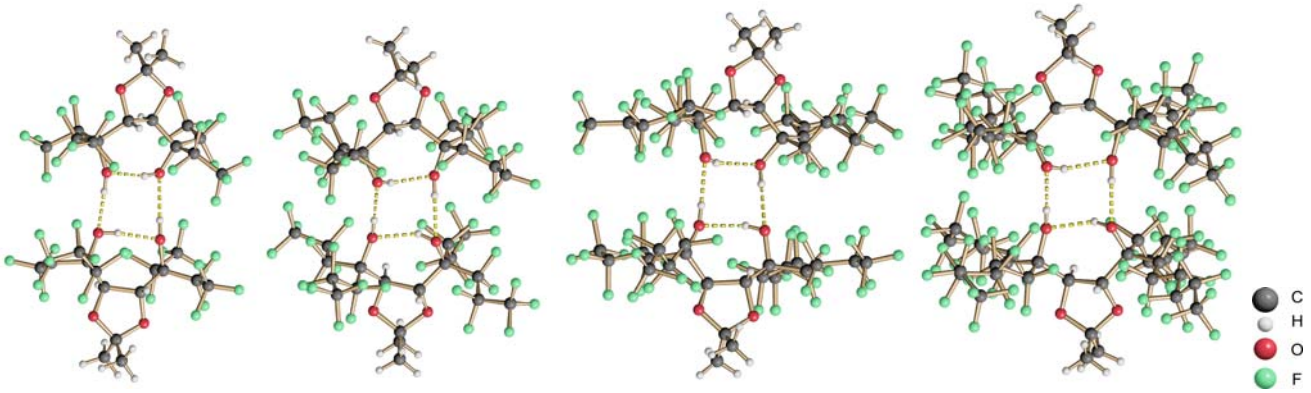

5b **5c** **5d** **5e**

of endless H-bonded aggregates (as in **5a**, Figure 7), and accounts for the observed change in packing. The higher TEFDDOL homologues **5d** and **5e** form dimers with an analogous hydrogen bonding pattern (Figure 8). Note that in the area of fluorinated mono-alcohols,

similar oligomers, with analogous 8-membered cyclic hydrogen bond networks, are observed e.g. for racemic 1-phenyl-2,2,2-trifluoro-ethanol.[10,20]

The crystal structure of the tetrakis-pentafluorophenyl-TEFDDOL **5f** revealed a completely different aggregation mode of the individual molecules. Unlike all other TEFDDOLs, and almost all TADDOLs which have an intramolecular O-H-O-hydrogen bond, this is not the case for the TEFDDOL **5f**. Instead, its hydroxyl groups are involved in both intra- and intermolecular O-H-F bonding (Figure 9).

Figure 9. Intra- and intermolecular OH-F hydrogen bonding in tetrakis-pentafluorophenyl-TEFDDOL **5f**.

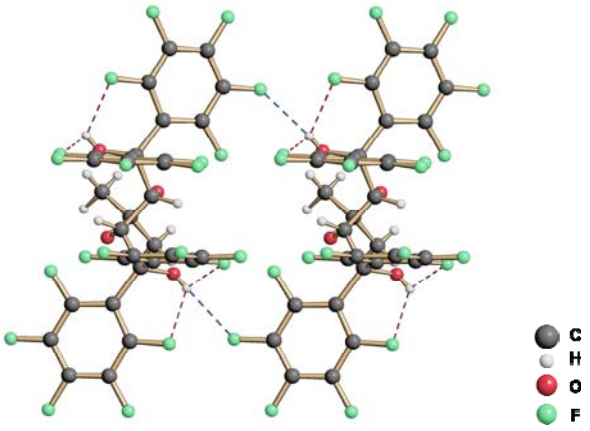

As mentioned before, each one of TEFDDOL **5f**'s hydroxyl group forms a bifurcated hydrogen bond to two "ortho" fluorine atoms on the phenyl rings (Figure 9, marked in red). In the crystal, a third - now intermolecular - interaction exists between the hydroxyl groups' H-atom and a "meta" fluorine atom of a neighboring TEFDDOL molecule (Figure 9, marked in blue). For the intermolecular OH-F bonds, the H-F distances were found to be in the range of 2.33-2.46 Å - significantly below the sum of the van der Waals radii of the two atoms (267

pm). Clearly, also the lengths of the intramolecular OH-F bonds in TEFDDOL **5f** (2.23-2.29 Å, see above) fall significantly below this value.

An earlier analysis of hydrogen bonding involving "organic" fluorine as acceptor (1997 by Dunitz and Taylor, based mainly on crystal structures) came to the conclusion that this type of interaction occurs only scarcely.[21] A very recent (2012) discussion of the topic by Schneider, including spectroscopy, association equilibria in solution, and computational studies, points to a much more widespread occurence and importance of hydrogen bonding to fluorine.[22] We feel that TEFDDOL **5f** is a good example for the importance of OH-F bonding, both with regard to molecular conformation and aggregation.

2.2.3 X-Ray crystal structures of the TEFDDOLs 5a-f in the presence of Lewis-bases: complexes with hydrogen bond acceptors.

Water as the second component: We also obtained crystallographic data of TEFDDOL **5a** as a 2:1 complex with water (Figure 10). In this hydrate, again an intramolecular hydrogen bond between the two hydroxyl groups of each TEFDDOL monomer is visible. Two TEFDDOL monomers dimerize, similar to the aggregation mode seen in water-free TEFDDOL **5a** (Figure 7). The terminal “activated” hydroxyl group of the dimer then forms an intermolecular hydrogen bond to water, which itself donates another intermolecular hydrogen bond to one of the oxygen atoms of the dioxolane ring of a TEFDDOL from the next TEFDDOL-dimer. Overall, an endless hydrogen bonded [**5a**$_2$-H_2O]$_n$-aggregate results (Figure 10). The crystal structure of the 2:1-complex of the tetrakis-pentafluoroethyl TEFDDOL **5b** with water revealed a rather similar hydrogen bonding pattern, giving rise to an endless [**5b**$_2$-H_2O]$_n$-aggregate (Figure 11).

Figure 10. 2:1-Complex of TEFDDOL **5a** with H_2O.

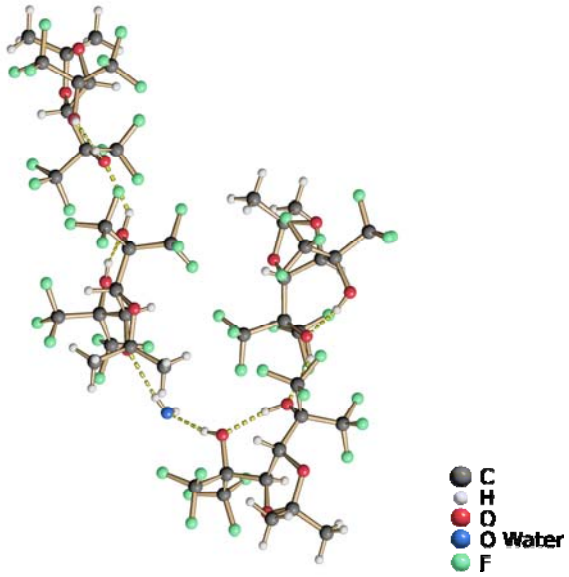

Figure 11. 2:1-Complex of TEFDDOL **5b** with H_2O.

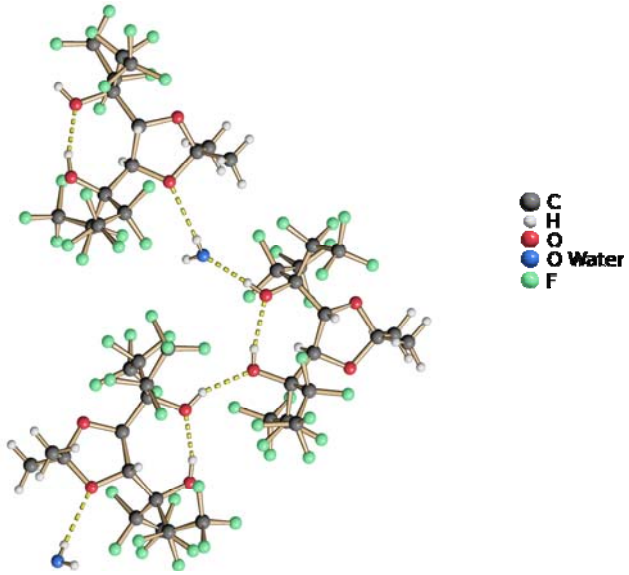

Amines (DABCO and piperidine) as the second component: In the cases of the pentafluoroethyl-TEFDDOL **5b** and the pentafluorophenyl-TEFDDOL **5f**, we have also

prepared and characterized complexes with amine bases, in particular with piperidine and DABCO (1,4-diazabicyclo[2.2.2]octane).

The crystal structure of the complex of **5b** with DABCO is shown in Figure 12. The composition of this material can be described as a [TEFDDOL-H^+•DABCO+H^+•TEFDDOL]-salt. As it should be the case, the tertiary diamine [pK_a(DMSO) = 8.93, 2.97][23] is mono-protonated by one of two tetrakis-pentafluoroethyl TEFDDOL (**5b**) molecules. Once again,

Figure 12. 2:1-Complex of TEFDDOL **5b** with DABCO.

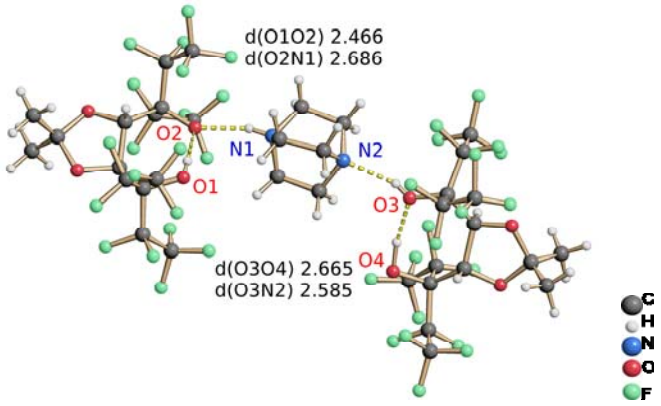

intramolecular H-bonds exist between the hydroxyl groups of the two TEFDDOL units [d_{O1O2} = 2.466(6) Å, d_{O3O4} = 2.655(8) Å]. It is evident from these bond lengths that one of the two TEFDDOL molecules is deprotonated, i.e. has transferred the “exocyclic” proton to the amine. In Figure 12, the deprotonated TEFDDOL unit is the “left” one, harbouring O1 and O2. The “right” TEFDDOL molecule appears to just form a strong hydrogen bond to the second N-atom of DABCO. Overall, two intermolecular hydrogen bonds exist between the N-atoms of DABCO and the “activated” hydroxyl groups of the two TEFDDOL molecules [d_{N1O2}=2.686(6) Å, d_{N2O3}=2.585(7) Å].

With DABCO as the proton acceptor, also the less acidic tetrakis-pentafluorophenyl-TEFDDOL **5f** forms a salt (Figure 13). In the 2:3-complex of C_6F_5-TEFDDOL **5f** with DABCO, we see two independent H-bridged ion pairs of DABCO+H^+• **5f**-H^+ (left and right in Figure 13). The relatively short O-O distances within the TEFDDOL moieties are indicative of the deprotonated state [d_{O1O2} = 2.562(3) Å, d_{O3O4} = 2.622(4) Å]. It is interesting to note that in the deprotonated state, the TEFDDOL **5f** adopts the conformation typical for all other TEFDDOLS, i.e. showing an intramolecular OH-O-hydrogen bond. In other words, single OH hydrogen bonding to the anionic carbinolate oxygen atom overrides two bifurcated OH-F hydrogen bonds. A third DABCO molecule occupies a central position as a non-hydrogen bonded guest molecule.

Figure 13. 2:3-Complex of TEFDDOL **5f** with DABCO.

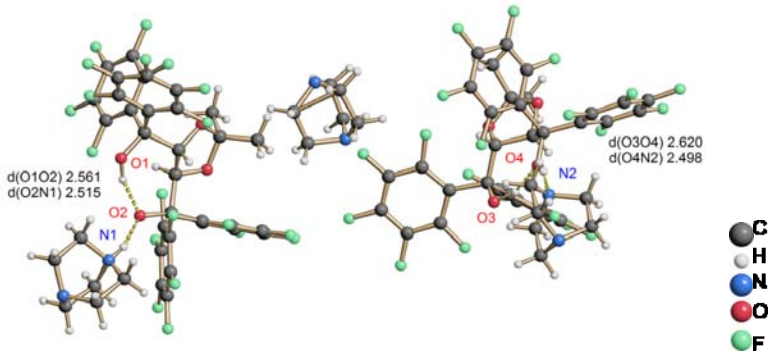

Not surprisingly, in the complex of the tetrakis-pentafluorophenyl-TEFDDOL **5f** with the more basic piperidine [pK_a(DMSO) = 10.85][24], the TEFDDOL is deprotonated as well (Figure 14). In this 2:1-complex, a cyclic hydrogen bond network is completed by incorporation of a second piperidine molecule. In this arrangement, the TEFDDOLs OH-O distance is short [d_{O1O2} = 2.457(3) Å], indicative of deprotonation of the TEFDDOL moiety.

Figure 14. 1:2-Complex of the tetrakis-pentafluorophenyl-TEFDDOL **5f** with piperidine (hydrogen atoms in the N-H-N-bridge are disordered).

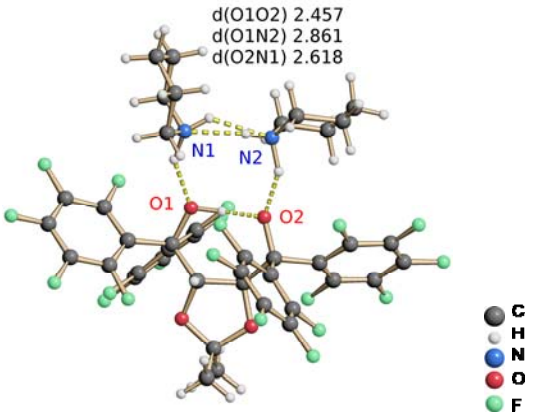

2.3 TEFDDOL-structures in solution.

The conformational and aggregational behaviour of the tetrakis-C_2F_5-TEFDDOL **5b** and of the tetrakis-C_6F_5-TEFDDOL **5f** (Figure 15) in solution was investigated by NOE- and by DOSY-spectroscopy, respectively (^{1}H, ^{19}F).

2.3.1 TEFDDOL-conformations in solution – NOE experiments.

For the tetrakis-C_2F_5-TEFDDOL **5b**, the "pseudo-syn" orientation of the intramolecularly hydrogen-bonded hydroxyl functions (see Figures 6,8) could be also confirmed for the solution structure of **5b** (Figure 16). In the homonuclear F,F NOESY spectrum, the two non-equivalent pentafluoroethyl groups can be assigned, while the H,F HOESY experiment served to distinguish between the two thinkable conformers for the signal set observed. In particular, the very strong cross peaks between H4/5 and $F2_{B''}$ - or H4/5 and $F1_{B''}$ – (see

Figure 15. Numbering scheme for TEFDDOLs **5b** and **5f** investigated by NMR spectroscopy.

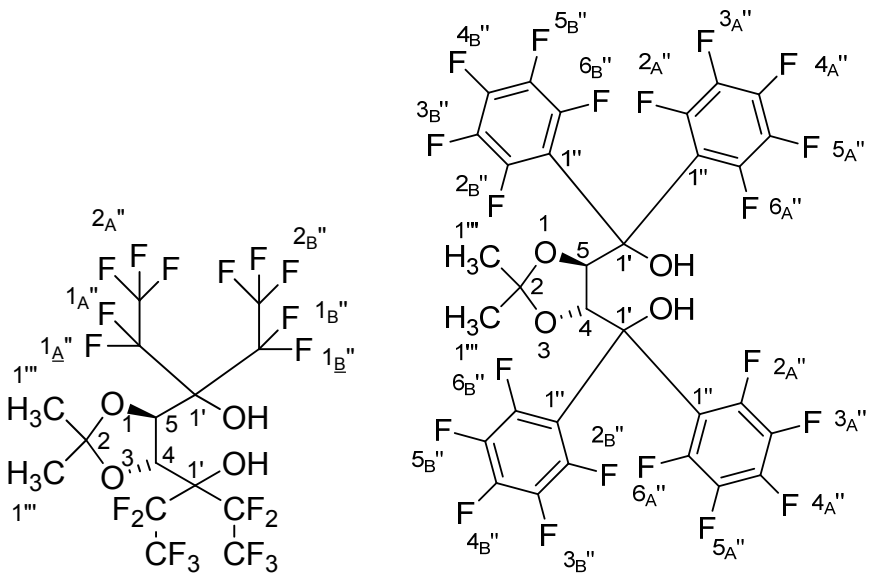

5b **5f**

Figure 15 for atom numbering) are not expected for a conformation where the two OH functionalities are pointing in opposite directions from the plane of the five-membered ring ("pseudo-anti"). On the contrary, no cross peak is observed between H4/5 and $F1_{A''}$ and only a very weak NOE between H4/5 and $F1_{A''}$, which cannot be accounted for by a "pseudo-anti" conformer. Likewise, the non-existence of a cross peak for H1''' and $F2_{B''}$ together with the strong NOE for H1''' and $F2_{A''}$ can only be explained with a "pseudo-syn" arrangement of the hydroxyl groups with respect to each other.

Figure 16. NOEs observed for the TEFDDOL **5b**. For reasons of clarity, the second **5b** molecule present in the dimeric aggregate is not shown. See Supporting Information for the original NOESY spectra.

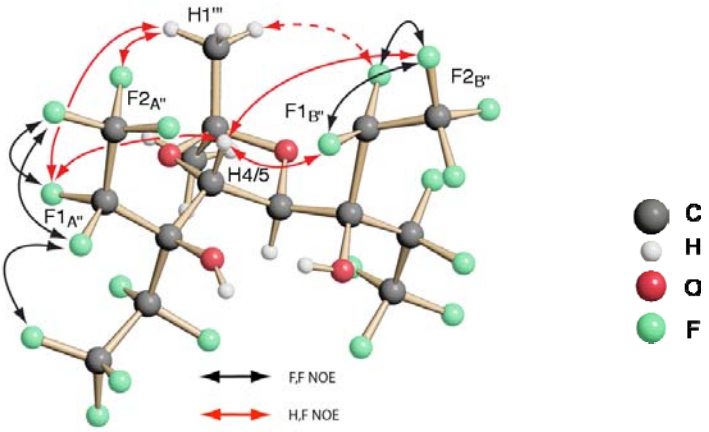

For the tetrakis-C_6F_5-TEFDDOL **5f** - as also indicated by diffusion measurements (see below) - a monomeric structure is supported by NOE data as well. Homo- and heteronuclear NOE experiment were performed. In particular, the two-dimensional H,F HOESY spectra show that in solution, like in the solid state (compare Figure 6), a “pseudo-anti” arrangement of the two OH-groups is preferred (Figure 17). In other words, also in $CDCl_3$ solution, the molecule's conformation is dominated by intramolecular OH-F bonding. Distance evaluation for possible “pseudo-syn” and “pseudo-anti” conformers, with the first one forming a possible dimer, and comparison with NOE data led to the assignment given in the Experimental Section. A very strong NOE between H4/5 and $F2_{B''}/F6_{B''}$, which is attributed to the NOE between each of the two identical stacked C_6F_5 unit’s interaction with the methine group, and also the strong NOE’s between the hydroxyl protons and $F2_{A''}/F6_{A''}$ and $F2_{B''}/F6_{B''}$, as well as H1''' and $F2_{A''}/F6_{A''}$ are in favor of this interpretation. At the same time, missing NOE contacts between H1''' and $F4_{B''}$ or $F3_{B''}/F5_{B''}$, respectively, clearly would be in contradiction with a “pseudo-syn” form and therefore further support our conclusions.

Figure 17. NOEs observed for the TEFDDOL **5f**. See Supporting Information for the original NOESY spectra.

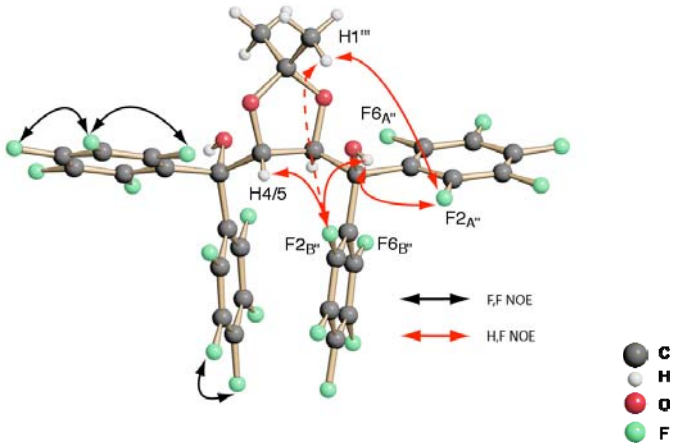

2.3.2 Supramolecular structures in solution – DOSY experiments.

For the tetrakis-pentafluoroethyl TEFDDOL **5b**, diffusion measurements were recorded for a series of different concentrations, ranging from 0.8 mM to 12.5 mM (in $CDCl_3$). As can be seen from the plot of diffusion coefficients vs. concentration (Figure 18), at diol concentrations below 0.01 M, an increase in diffusion coefficient - which is equivalent to a larger fraction of monomeric species - can be observed. As has been suggested earlier, changes in hydrodynamic radii upon build-up or breaking of H-bonds can be gauged by using TMS as an internal diffusion reference.[25] By comparison of experimentally determined diffusion coefficients and the relative change in hydrodynamic radius, the value of D/D^{TMS} of ca. 0.5 for the concentrations of 12.5 mM and above, vs. D/D^{TMS} of 0.73 for the most diluted solution under investigation, and a corresponding change of the hydrodynamic radius, Δr_H, by ca. 1.4, were obtained. This result can be interpreted by the TEFDDOL **5b** existing in an aggregation state close to monomer in solutions of ca. 0.8 mM in concentration, or below.

Note that this value was determined in chloroform as solvent which is at the most of very low hydrogen bond accepting capacity. We interpret the aggregation state being populated at higher concentrations as the H-bonded dimer found in the crystal structure of TEFDDOL **5b** (Figure 8).

Figure 18. TEFDDOL **5b**: diffusion coefficient in $CDCl_3$ as a function of concentration. TMS was used as standard. See Supporting Information.

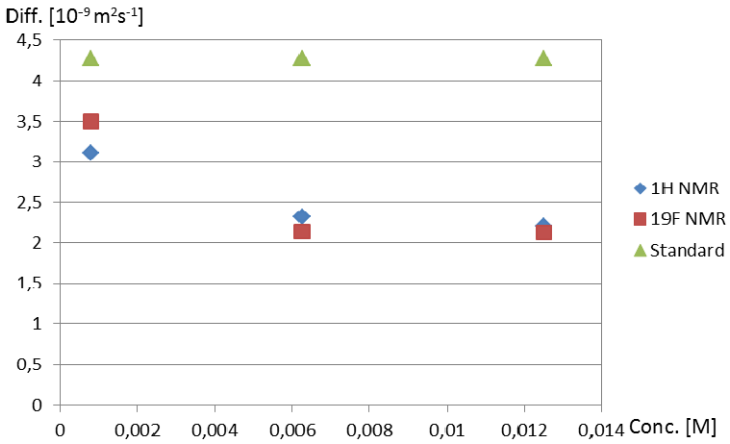

A similar set of diffusion experiments was carried for the tetrakis-pentafluorophenyl-TEFFDOL **5f**. In contrast to the changes observed for increasingly diluted solutions of the TEFDDOL **5b**, when recording diffusion experiments with **5f**, almost no changes in diffusion coefficient were visible throughout the investigated range of concentrations (Figure 19). At the same time, the absolute values of diffusion coefficients match the ones expected for the monomeric TEFDDOL **5f** in chloroform solution. In other words, the tetrakis-pentafluorophenyl-TEFDDOL **5f** does not show any tendency towards aggregation in chloroform solution up to at least 12.5 mM concentration. This result indicates that the third

and intermolecular OH-F hydrogen bond found in the crystal structure of **5f** (Figure 9, H-bonds indicated in blue) is weak and does not persist in solution.

Figure 19. TEFDDOL **5f**: diffusion coefficient in $CDCl_3$ as a function of concentration. TMS was used as standard. See Supporting Information.

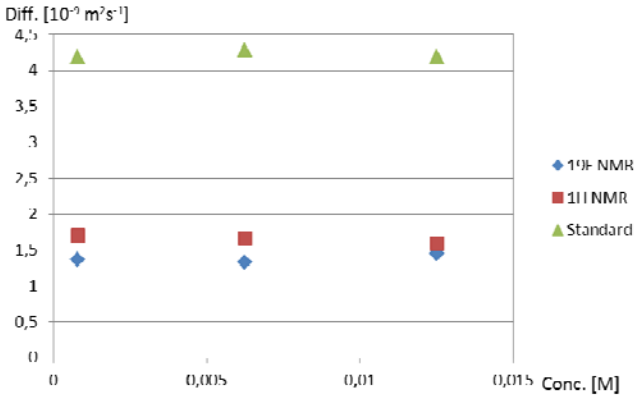

2.4. Miscellaneous.

2.4.1 The attempted synthesis of the *meso*-TEFDDOL 9. Under the same reaction condition as described above (2.1.2), we have tried to synthesize an achiral counterpart of the tetrakis-pentafluoroethyl TEFDDOL **2b**, namely the *meso*-TEFDDOL **9** (Figure 20). For

Figure 20. Formulae of the desired *meso*-TEFDDOL **9** and of *iso*-propylidene *meso*-tartaric anhydride **10**.

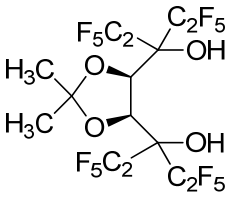

9

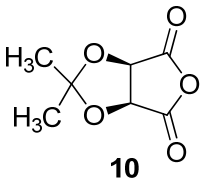

10

the preparation of the required *meso*-tartaric dichloride, we applied the procedure by Klotz et al. for the synthesis of the chiral tartaric dichloride **7**.[17] However, treatment of the *meso*-tartaric disodium salt with thionyl chloride furnished the anhydride **10**, which was employed for further experimentation.

As described under 2.1.2, pentafluoroethyl iodide and the anhydride **10** were dissolved in diethylether at -78°C, and methyl lithium, stabilized with lithium bromide was added. Under these conditions, no indication for the formation of the desired *meso*-TEFDDOL **9** was obtained. Instead, the product *rac*-**11** with only two pentafluoroethyl groups was isolated (Scheme 3).

Scheme 3. Synthesis of compound rac-**11** starting from *iso*-propylidene protected anhydride **10**.

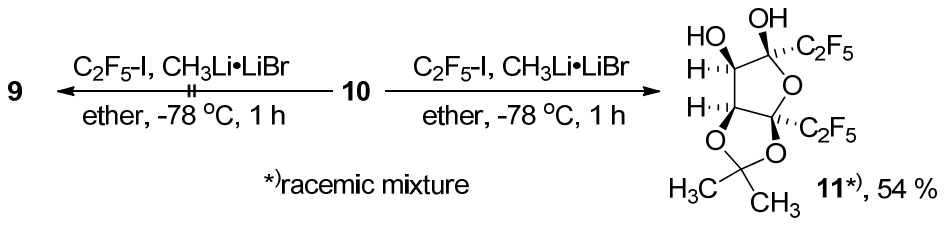

The X-ray crystal structure of *rac*-**11** is shown in Figure 21. In the crystal, the enantiomers of *rac*-**11** form heterochiral hydrogen-bonded dimers ("horizontal" hydrogen bonds in Figure 21). The latter dimers aggregate, again by hydrogen bonding ("vertical" H-bonds in Figure 21), to endless ribbons.

Figure 21. X-Ray crystal structure of compound *rac*-**11**: molecular structure (top); intermolecular hydrogen bonding pattern (bottom).

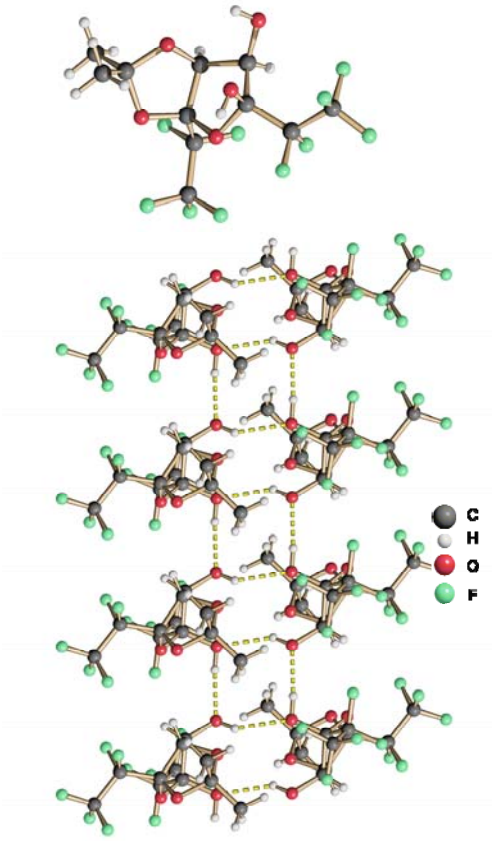

The formation of the unexpected product *rac*-**11** from the *meso*-tartaric anhydride **10** can be explained as summarized in Scheme 4. Initial *exo*-attack of pentafluoroethyllithum on the bicyclic anhydride **10** affords the alcoholate *rac*-**12**. A second *exo*-attack on the remaining carbonyl group furnishes the diolate *meso*-**13**. As the final step, trans-acetalization – most likely during acidic workup - in *meso*-**13** affords *rac*-**11**. The latter process is facilitated by the *cis*-orientation of the hydroxyl groups involved.

Scheme 4. Suggested mechanism for the formation of the diol *rac*-**11**.

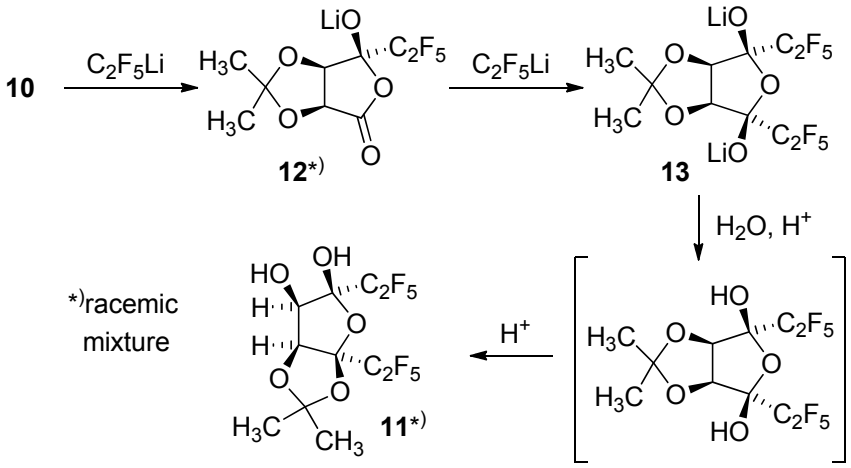

2.4.2. pK_a-Values of the TEFDDOLs 5a,b,f. We recently disclosed the pK_a values of the TEFDDOLs **5a**, **5b** and **5f** in DMSO.[11] It was found that the tetrakis-perfluoralkyl-TEFDDOLs **5a** and **5b** are rather acidic [pK_a (**5a**) = 5.7; pK_a (**5b**) = 2.4], wheras the tetrakis-pentafluorophenyl-TEFDDOL **5f** has a pK_a value of ca. 11. Clearly, intramolecular hydrogen bonding accounts for the increased acidity of the tetrakis-perfluoroalkyldiols **5a** and **5b** relative to their "monomer" 1,1,1,3,3,3-hexafluoro-2-propanol (HFIP, pK_a = 17.2[11]). In the case of the tetrakis-pentafluorophenyl-TEFDDOL **5f**, the pK_a of ca. 11 is basically identical to that of the "monomer" decafluorohenzhydrol (ca.11).[11] In other words, the hydroxyl groups of **5f** act independently - consistent with TEFDDOL **5f**'s preferred "pseudo-anti"-conformation, both in the crystal (Figures 6 and 9) and in solution (Figure 17).

3. Conclusions

(i) We have established a versatile one-step synthesis for a novel class of chiral and highly fluorinated diols, the TEFDDOLs (α,α,α',α'-tetrakisperfluoroaryl/alkyl-5,5'-dimethyl-1-3-dioxolan-4,5-dimethanols).

(ii) All perfluororalkyl-TEFDDOLs (**5a**-**e**) show intramolecular HO-HO hydrogen bonding, both in the solid state and in solution ("pseudo-syn" orientation of the H-bonded OH groups). As a result, the perfluoroalkyl TEFDDOLs show acidity significantly higher than the parent fluorinated mono-alcohols. pK_a-Values as low as 2.4 were measured, which make the TEFDDOLs promising candidates for applications in asymmetric organocatalysis.

(iii) In the tetrakis-pentafluorophenyl-TEFDDOL **5f**, the overall conformation is dictated by bifurcated intramolecular hydrogen bonding between the molecule's OH groups and the "ortho" fluorine atoms of the C_6F_5-rings. This interaction overrides the molecules's intrinsic potential for intramolecular HO-HO hydrogen bonding, and a "pseudo-anti" arrangement of the OH groups results. As a consequence of the non-cooperativity of its OH-groups, the tetrakis-pentafluorophenyl-TEFDDOL **5f** does not show enhanced acidity relative to its mono-alcohol decafluorobenzhydrol.

(iv) In the solid state, the pure perfluororalkyl-TEFDDOLs **5a**-**e** form aggregates (dimers to infinite ribbons) by intermolecular hydrogen bonding. Furthermore, these aggregates are characterized by a strict layering of the perfluoroalkyl groups, the highly polar OH-groups, and the dioxolane residues of medium polarity.

(v) An analogous layering is observed for the tetrakis-pentafluorophenyl-TEFDDOL **5f**. Intermolecular bonding, however, is effected by weak OH-F interactions, and not by HO-HO bonds.

(vi) In chloroform solution, the conformational features found in the crystal for both the perfluoroalkyl- and perfluorophenyl-TEFDDOLs **5b** and **5f** persist. The monomeric tetrakis-perfluoroethyl-TEFDDOL **5b** is in equilibrium with a dimer which prevails at higher

concentrations. In contrast, the tetrakis-perfluoropheny-TEFDDOL **5f** shows no tendency towards aggregation.

(vii) In the presence of Lewis-bases (water, amines), all TEFDDOLs form well-defined aggregates in the solid state. The TEFDDOL's diol substructure acts as "monodentate" hydrogen bond donor.

(viii) In the presence of sufficiently basic partners (amines), the TEFDDOLs may become deprotonated and can form crystalline ammonium salts. For the tetrakis-pentafluorophenyl-TEFDDOL **5f**, deprotonation is accompanied by a dramatic change in conformation: in its anion, OH-F hydrogen bonding is overridden, and a conformation with an intramolecular OH-O hydrogen bond results (i.e. the conformation typical for all tetrakis-perfluoroalkyl-TEFDDOLs).

Future studies in our laboratory will be devoted to potential applications of this new class of chiral fluorodiols, in particular with regard to their potential as chiral Brønsted acids, or building blocks for chiral ligands.

4. Experimental Section

4.1. General Information. All reactions were carried out under argon atmosphere and in flame-dried glassware, using standard Schlenk techniques. Reagents were purchased from standard suppliers and were used without further purification. Solvents were dried according to general procedures.[26] TLC spots were visualized by fluorescent indicator or by cerium-molybdenum-spray reagent. Flash chromatography was performed on silica gel. Gas chromatography (GC): Helium was used as a carrier gas, and HP-5 MS or Optima 5 Accent (Macherey-Nagel) 30 m x 0.25 mm capillary columns. GC-data are given as follows: type of

the column, GC-method in the following formula: initial temperature [min] → ramp [°C/min] → final temperature [min].

Nuclear magnetic resonance (NMR): ^{1}H and ^{13}C chemical shifts (δ) are given in ppm relative to the solvent reference as an internal standard. Assignments are supported by H,H COSY, H,C HMQC and H,C HMBC spectra. Gradient-selected F,F COSY, F,C HMBC and H,F HOESY[27] spectra were recorded using an inverse H,F TBI probe, equipped with a pulsed gradient unit capable of producing magnetic field pulse gradients in the z-direction of 56 G•cm^{-1}. Data are reported as follows: chemical shift [multiplicity (s for singlet, d for dublet, t for triplet, q for quartet, sept for septet, m for multiplet), coupling constant [Hz], integration, assignment]. For the attribution of scalar couplings, ^{19}F NMR spectra were simulated with SpinWorks 3.1.7 (Copyright 2010, K. Marat, University of Manitoba) using NUMRIT algorithms.[28] For the numbering scheme of ^{19}F NMR assignments, see Figure 15.

High-resolution mass spectrometry (HR-MS): High-resolution mass spectra were recorded in ESI mode, using a quadrupole ion trap (EB-Q-trap).

Fourier transform infrared spectroscopy (FT-IR): Absorption bands are given in wave numbers ($\tilde{\nu}$, cm^{-1}). Intensities of the bands are given as follows: ‘s’ for strong peaks, ‘m’ for peaks with a medium intensity and ‘w’ for weak bands. Broad absorptions are marked with supplement ‘br’.

Melting points (m.p.) are uncorrected.

X-ray crystal structure analysis: Structures were solved using SHELXS97, and refined with SHELXL97.

For *optical rotations*, concentrations c are given in g/100 ml.

4.2 Preparation of the acid chloride 7 and anhydride 10.

(4R,5R)-2,2-Dimethyl-1,3-dioxolan-4,5-dicarbonyl dichloride (7). This acid chloride was prepared according to Klotz et al. (ref. 17). Yield (from 1.00 g of the disodium salt): 780 mg (3.45 mmol, 81 % Lit.: 69 %), colorless crystals were obtained by sublimation (10^{-2} mbar, 50 ^{o}C); m.p. 40--42 °C. ^{1}H NMR (300.1 MHz, $CDCl_3$): δ 5.20 (s; 2H), 1.56 (s; 6H). ^{13}C NMR (75.5 MHz, $CDCl_3$): δ 172.1, 117.4, 83.7, 26.8. ESI-MS (pos.): m/z (%) = 227 (11) [M^+]. IR: $\tilde{\nu}$ = 2993 (w), 2945 (w), 1776 (s), 1455 (w), 1377 (m), 1230 (m), 1122 (m), 1008 (m), 982 (w), 954 (w), 825 (w), 746 (w), 695 (w), 652 (w), 599 (w) cm^{-1}.

X-ray structural data of **7** (CCDC 827655): $C_7H_8Cl_2O_4$, formula weight 227.03, crystal size 0.30 x 0.20 x 0.10 mm, crystal system monoclinic, space group C2, unit cell dimensions *a* = 14.2526 (12), *b* = 8.9791 (10) Å, *c* = 9.7106 (5) Å, *β* = 129.481 (4)°, *Z* = 4, *D*calcd. 1.572 gcm^3, absorption coefficient 0.655 mm^{-1}, wavelength 0.71073 Å, *T* = 100 (2) K, $2\theta_{max}$ = 27.00°, reflections collected/unique 35033/9028 [*R*(int) = 0. 0202], final *R* indices [$I > 2\sigma(I)$] *R* = 0.0301, *wR* = 0.0652, largest diff. peak and hole 0.219 and -0.290 $eÅ^{-3}$.

(3aR,6aS)-2,2-Dimethylfuro[3,4-d][1,3]dioxole-4,6-(3aH, 6aH)-dione (10). This acid anhydride was prepared analogous to the procedure by Klotz et al. (ref. 17). Yield (from 1.50 g of the disodium salt): 510 mg (1.97 mmol, 46 %), colorless crystals were obtained by sublimation (10^{-2} mbar, 60 ^{o}C); m.p. 49-51 °C. ^{1}H NMR (300.1 MHz, $CDCl_3$): δ 5.16 (s; 2H), 1.51 (s; 6H). ^{13}C NMR (75.5 MHz, $CDCl_3$): δ 172.1, 117.4, 83.7, 26.9. GCMS: τ_R = 14:61 min; m/z = 207, 189, 176, 158, 145, 129, 115, 101, 85, 73, 59; Macherey Optima-5MS; 35 °C, 5 min, 20 °C/min → 280 °C, 10 min. ESI-MS (pos.): m/z (%) = 195 [M^+ +Na^+] (16), 173 [M^++H^+] (100). IR: $\tilde{\nu}$ = 3534 (w), 3312 (br), 2822 (br), 2623 (br), 2488 (br), 1713 (s), 1682 (s), 1439

(m), 1306 (m), 1252 (m), 1207 (s), 1125 (m), 1098 (s), 914 (m), 874 (m), 822, (m) 743 (m) cm^{-1}.

X-ray structural data of **10** (CCDC 827664): $C_7H_8O_5$, formula weight 172.13, crystal size 0.40 x 0.40 x 0.15 mm, crystal system monoclinic, space group $P2_1/c$, unit cell dimensions *a* = 8.7026 (10) Å, *b* = 7.6311 (8) Å, *c* = 11.557 (2) Å, *β* = 103.131° (4), *Z* = 4, *D*calcd. 1.530 gcm^{-3}, absorption coefficient 0.133 mm^{-1}, wavelength 0.71073 Å, *T* = 100 (2) K, $2\theta_{max}$ = 27.00°, reflections collected/unique 3691/1630 [*R*(int) = 0.0407], final *R* indices [$I > 2\sigma(I)$] *R* = 0.0349, *wR* = 0.0762, largest diff. peak and hole 0.171 and -0.228 $eÅ^{-3}$.

4.3 Preparation of the tetrakis-trifluoromethyl-TEFDDOL 5a and of the carboxylic acid 8 by using Ruppert's reagent (6).

[(4R,5R)-2,2-Dimethyl-1,3-dioxolane-4,5-diyl]bis(1,1,1,3,3,3-hexafluoro-propan-2-ol) (5a). The tartaric acid dichloride **7** (1.00 g, 1.00 equiv, 4.30 mmol) was dissolved in 25 mL of glyme, and the solution was cooled to -50 °C. Trimethyl(trifluoromethyl)silane (**6**) (4.65 mL, 7.10 equiv, 31.42 mmol) and tetramethylammonium fluoride (TMAF, 2.93 g, 7.10 equiv, 31.42 mmol) were added at -50°C. The reaction mixture was stirred for 1 h at -30 °C and then overnight at room temperature. Saturated aq. NH_4Cl was added (30 mL). The layers were separated, and the aqueous phase was extracted with diethyl ether. The combined organic extracts were dried over $MgSO_4$, and the solvent was evaporated in vacuo. The crude product (yellowish brown oil) was purified by flash chromatography (cyclohexane/EtOAc 1:1) and subsequent sublimation or crystallization to give the trifluoromethylated reaction product **5a** as colorless crystals.

Water-free colorless crystals (374 mg, 20 %) were obtained by sublimation at 50 °C under vacuum (10^{-2} mbar) in a sealed tube, and through a layer of 4 Å molecular sieves; m.p.; 104-105 °C. $[\alpha]_D^{20}$ +4.6 (*c* 0.6, $CHCl_3$). ^{1}H NMR (300.1 MHz, $CDCl_3$): δ 4.78 (s; 2H), 1.48 (s; 6H), OH not detected. ^{13}C NMR (75.5 MHz, $CDCl_3$): δ 122.2, 121.5, 113.9, 78.1, 75.2, 26.6. ^{19}F NMR: (282.4 MHz, $CDCl_3$): δ -71.45 (q; 6F, F-1_A",$^4J_{FF}$ = 9.0 Hz), 75.89 (q; 6F, F-1_B", $^4J_{FF}$ = 9.0 Hz). GCMS: τ_R = 8.55 min; m/z = 420, 419, 395, 267, 251, 238, 169, 147, 121, 97, 91, 85, 78, 69, 59, 55; Macherey Optima-5MS; 35 °C, 5 min, 20 °C/min → 280 °C, 10 min. ESI-MS (neg.): m/z (%) = 433 [M-H$^+$] (99). IR: ῡ = 3269 (br), 2999 (w), 2963 (w), 1674 (w), 1468 (w), 1379 (w), 1279 (w), 1244 (w), 1244 (s), 1204 (s), 1146 (s), 1128 (s), 1090 (s), 1065 (m), 1053 (m), 1034 (m), 982 (m), 957 (m), 880 (m), 810 (m), 799 (m), 737 (m), 721 (m), 689 (w), 660 (w), 625 (w), 606 (w) [cm^{-1}]. Elemental analysis calcd (%) for $C_{11}H_{10}F_{12}O_4$ (434.31): C 30.43 %, H 2.32 %; found: C 30.29 %, H 2.21 %.

X-ray structural data **5a** (CCDC 798769): Water-free crystals of **5a**, suitable for X-ray crystallography, were obtained by sublimation at 50 °C under vacuum (10^{-2} mbar) in a sealed tube, and through a layer of 4 Å molecular sieves. $C_{11}H_{10}F_{12}O_4$, formula weight 434.31 , crystal size 0.20 x 0.20 x 0.10 mm, crystal system orthorhombic, space group $P2_12_12_1$, unit cell dimensions *a* = 9.9444 (5) Å, *b* = 13.0012 (7) Å, *c* = 36.1469 (3) Å, *Z* = 12, *D*calcd. 1.851 gcm^{-3}, absorption coefficient 0.226 mm^{-1}, wavelength 0.71073 Å, *T* = 100 (2) K, $2\theta_{max}$ = 27.00°, reflections collected/unique 18993/9372 [*R*(int) = 0.05565], final *R* indices [$I > 2\sigma(I)$] *R* = 0.0437, *wR* = 0.0661, largest diff. peak and hole 0.305 and -0.325 $eÅ^{-3}$.

(4R,5R)-5-(1,1,1,3,3,3-Hexafluoro-2-hydroxypropan-2-yl)-2,2-dimethyl-1,3-dioxolane-4-carboxylic acid (8). Analogously, 0.43 g (1.92 mmol, 1.00 equiv) of the acid chloride **7** were

reacted with 1.16 mL (7.68 mmol, 5.00 equiv) of CF_3-TMS (**6**) and 0.72 g (7.68 mmol, 5.00 equiv) of TMAF.

Colorless crystals (200 mg, 33 %) were obtained by crystallisation from DCM; m.p. 70-72 °C. ^{1}H NMR (300.1 MHz, $CDCl_3$): δ 11.0 (s; 1H, OH), 6.45 (s; 1H, OH), 4.78 (d; 1H, ^3J = 7.0 Hz), 4.77 (d; 1H, ^3J = 7.0 Hz), 1.47 (s; 3H), 1.56 (s; 3H). ^{13}C NMR (75.5 MHz, $CDCl_3$): δ 174.8, 120.1, 116.4, 113.7, 76.9, 76.5, 76.2, 26.1, 25.8. ^{19}F NMR: (282.4 MHz, $CDCl_3$): δ 72.88 (q; 3F, $^4J_{FF}$ = 9.1 Hz), 75.96 (q; 3F, $^4J_{FF}$ = 9.1 Hz). GCMS: τ_R = 10.13 min; m/z = 298, 297, 267, 251, 227, 169, 145, 128, 97, 91, 85, 78, 69, 59, 55; Macherey Optima-5MS; 35 °C, 5 min, 20 °C/min → 280 °C, 10 min. ESI-MS (neg.): m/z (%) = 311 [M-H$^+$] (99). HRMS (ESI-): calcd. for $C_9H_{10}F_6O_5$ (anion): 311.03487; found: 311.03543 (error < 2 ppm). IR: $\tilde{\upsilon}$ = 3325 (br), 2999 (w), 2359 (w), 2332 (w), 1836 (w), 1734 (m) 1628 (w), 145 (w), 1379 (w), 1361 (w), 1210 (s), 1148 (s), 1082 (s) 1034 (w), 978 (w), 959 (w), 866 (w), 799 (w), 719 (w), 685 (w), 654 (w) [cm^{-1}].

X-ray structural data of **8** (CCDC 866491): $C_9H_{10}F_6O_5$, formula weight 312.16, crystal size 0.15 x 0.15 x 0.02 mm, crystal system monoclinic, space group $P2_1$, unit cell dimensions a = 9.47 (2) Å, b = 6.580 (10) Å, c = 10.22 (3) Å, β = 106.01 (6)°, Z = 2, Dcalcd. 1.695 gcm^{-3}, absorption coefficient 0.190 mm^{-1}, wavelength 0.71073 Å, T = 100 (2) K, $2\theta_{max}$ = 24.99°, reflections collected/unique 1282/1094 [R(int) = 0.0519], final R indices [I >2σ(I)] R = 0.0568, wR = 0.1200, largest diff. peak and hole 0.196 and -0.215 eÅ^{-3}.

4.4 General procedure for the preparation of the TEFDDOLs (α,α,α',α'-tetrakisperfluoroalkyl/aryl-2,2'-dimethyl-1-3-dioxolane-4,5-dimethanols) 5b-f by halogen-lithium exchange. (R,R)-*iso*-Propylidene tartaric dichloride (7; 500 mg, 2.2 mmol,

1.00 equiv.) and the perflourinated alkyl/aryl iodide or bromide (7.10 equiv., 15.6 mmol) were dissolved in 30 mL of dry diethyl ether at -78°C, and methyllithium, stabilized with lithium bromide (1.5 M in diethyl ether, 7.33 mL, 11.00 mmol, 5.00 equiv.) was slowly added. The reaction mixture was stirred for 1 h at -78°C and subsequently quenched by addition of saturated aq. NH_4Cl (30 mL). The layers were separated, and the aqueous phase was extracted with diethyl ether. The combined organic phases were dried over $MgSO_4$, and the solvent was evaporated in vacuo. The crude product (yellowish-brown oil) was purified by flash chromatography (cyclohexane/EtOAc 1:1) and subsequent sublimation or crystallisation to give the tetrakisperfluoroalkyl/aryl-TEFDDOL as colorless crystals.

(4R,5R)-2,2-Dimethyl-4,5-[bis-(diperfluoroethyl-hydroxymethyl)]-1,3-dioxolane (5b). Pentafluoroethyliodide was used, colorless crystals (767 mg, 55 %) of the product **5b** were obtained by sublimation (10^{-2} mbar, 50 ^{o}C); m.p. 81-82 °C; $[\alpha]_D^{20}$ +4.1 (*c* 1.0, $CHCl_3$). ^{1}H NMR (300.1 MHz, $CDCl_3$): δ 4.86 (s; 2H), 1.44 (s; 6H), OH not detected. ^{13}C NMR (75.5 MHz, $CDCl_3$): δ 118.2, 118.3, 114.1, 119.9, 112.1, 78.1, 76.2, 25.8. ^{19}F NMR: (282.4 MHz, $CDCl_3$): δ -78.56 (dd; $^3J_{FF}$ = 16 Hz, $^3J_{FF}$ = 16 Hz, 6F, F-2$_A$"), -78.96 (dd; $^3J_{FF}$ = 2.5 Hz, $^3J_{FF}$ = 2.9 Hz, 6F, F-2$_B$"), 113.08 (m; $^2J_{FF}$ = 290 Hz, $^3J_{FF}$ = 2.5 Hz, $^4J_{FF}$ = 6.7 Hz, $^4J_{FF}$ = 6.7 Hz, 2F, F-1$_B$"), -114.32 (m; $^2J_{FF}$ = 290 Hz, $^3J_{FF}$ = 2.9 Hz, $^4J_{FF}$ = 12 Hz, $^4J_{FF}$ = 12 Hz, 2F, F-1$_{\underline{B}}$"), -118.14 (m; $^2J_{FF}$ = 150 Hz, $^3J_{FF}$ = 16 Hz, $^4J_{FF}$ = 12 Hz, $^4J_{FF}$ = 6.7 Hz, 2F, F-1$_A$"), 118.26 (m; $^2J_{FF}$ = 150 Hz, $^3J_{FF}$ = 16 Hz, $^4J_{FF}$ = 12 Hz, $^4J_{FF}$ = 6.7 Hz, 2F, F-1$_{\underline{A}}$"). GCMS: τ_R = 4.13 min; m/z = 516, 499, 367, 219, 171, 147, 119, 109, 85, 69, 59; Macherey Optima-5MS; 35 °C, 5 min, 20 °C/min → 280 °C, 10 min. ESI-MS (neg.): m/z (%) = 633 [M-H+] (99). IR: ν 3390 (br), 2920 (w), 1381 (w), 1327 (w), 1306 (w), 1218 (m), 1162 (m), 1058 (m), 990 (m), 865 (m), 740(m), 718 (m),

623 (w) [cm^{-1}]. Elemental analysis calcd. (%) for $C_{15}H_{10}F_{20}O_4$ (634.21): C 28.41 %, H 1.59 %; found: C 28.54 %, H 1.58 %.

X-ray structural data of **5b** (CCDC 866492): $C_{15}H_{10}F_{20}O_4$, formula weight 634.21, crystal size 0.20 x 0.20 x 0.10 mm, crystal system triklin, space group P1, unit cell dimensions *a* = 8.4682 (4) Å, *b* = 10.9244 (4) Å, *c* = 13.2571 (5) Å, α = 108.543 (2)°, β = 100.404 (2)°, γ = 104.790 (2)°, *Z* = 2, *D*calcd. 1.955 gcm^{-3}, absorption coefficient 0.249 mm^{-1}, wavelength 0.71073 Å, *T* = 100 (2) K, $2\theta_{max}$ = 26.99°, reflections collected/unique 9375/4699 [*R*(int) = 0.0233], final *R* indices [$I > 2\sigma(I)$] *R* = 0.0477, *wR* = 0.1126, largest diff. peak and hole 0.352 and -0.415e$Å^{-3}$.

(4R,5R)-2,2-Dimethyl-4,5-[bis-(diperfluoro-*n*-propyl-hydroxymethyl)]-1,3-dioxolane (5c). Heptafluoro-*n*-propyliodide was used, colorless crystals (459 mg, 25 %) of the product **5c** were obtained by sublimation (10^{-2} mbar, 50 °C) or crystallization from *n*-pentane; m.p. 132-133 °C; $[\alpha]_D^{20}$ +4.0 (*c* 0.99, $CHCl_3$). ^{1}H NMR (300.1 MHz, $CDCl_3$): δ 5.02 (s; 2H), 1.46 (s; 6H), OH not detected. ^{13}C NMR (75.5 MHz, $CDCl_3$): δ 117.8 (s; C-3A"), 117.6 (s; C-3B"), 109.8, 117.8-109.8, 114.9, 80.8, 76.9, 26.2. ^{19}F NMR (282.4 MHz, $CDCl_3$): δ -82.18 (dd; $^4J_{FF}$ = 12.5 Hz, $^4J_{FF}$ = 12.5 Hz, 6F, F-3_B"), -82.36 (dd; $^4J_{FF}$ = 12.5 Hz, $^4J_{FF}$ = 12.5 Hz, 6F, F-3_A"), 110.41 (m; $^2J_{FF}$ = 300 Hz, $^3J_{FF}$ = 21.0 Hz, $^3J_{FF}$ = 9.0 Hz, $^4J_{FF}$ = 12.5 Hz, $^4J_{FF}$ = 11.0 Hz, $^4J_{FF}$ = 5.0 Hz, 2F, F-1_A"), 111.11 (m; $^2J_{FF}$ = 300 Hz, $^3J_{FF}$ = 20.0 Hz, $^3J_{FF}$ = 8.0 Hz, $^4J_{FF}$ = 12.5 Hz, $^4J_{FF}$ = 8.0 Hz, $^4J_{FF}$ = 5.0 Hz, 2F, F-$1_{\underline{A}}$"), -113.67 (m; $^2J_{FF}$ = 295 Hz, $^3J_{FF}$ = 4 Hz, $^3J_{FF}$ = 2 Hz, $^4J_{FF}$ = 12.5 Hz, $^4J_{FF}$ = 11.0 Hz, $^4J_{FF}$ = 8.0 Hz, 2F, F-1_B"), -114.99 (m; $^2J_{FF}$ = 295 Hz, $^3J_{FF}$ = 5 Hz, $^3J_{FF}$ = 3 Hz, $^4J_{FF}$ = 12.5 Hz, $^4J_{FF}$ = 11.0 Hz, $^4J_{FF}$ = 8.0 Hz, 2F, F-$1_{\underline{B}}$"), -122.52 (m; $^2J_{FF}$ = 295 Hz, $^3J_{FF}$ = 21.0 Hz, $^3J_{FF}$ = 8.0 Hz, $^5J_{FF}$ = 5 Hz, $^5J_{FF}$ = 2 Hz, 2F, F-2_A"), 122.63 (m; $^2J_{FF}$ = 295 Hz, $^3J_{FF}$ =

20 Hz, $^{3}J_{FF}$ = 9 Hz, $^{5}J_{FF}$ = 4 Hz, $^{5}J_{FF}$ = 3 Hz, 2F, F-2$_{\underline{A}}$"), -124.59 (m; $^{2}J_{FF}$ = 292 Hz, $^{3}J_{FF}$ = 5 Hz, $^{3}J_{FF}$ = 2 Hz, $^{5}J_{FF}$ = 21 Hz, $^{5}J_{FF}$ = 8 Hz, 2F, F-2$_{B}$"), -125.04 (m; $^{2}J_{FF}$ = 292 Hz, $^{3}J_{FF}$ = 4 Hz, $^{3}J_{FF}$ = 3 Hz, $^{5}J_{FF}$ = 20 Hz, $^{5}J_{FF}$ = 9 Hz, 2F, F-2$_{\underline{B}}$"). GCMS: τ_R = 10.33 min; m/z = 467, 451, 421, 409, 373, 347, 297, 269, 251, 241, 221, 197, 169, 159, 131, 119, 100, 85, 69, 59; Macherey Optima-5MS; 35 °C, 5 min, 20 °C/min → 280 °C, 10 min; ESI-MS (neg.): m/z (%) = 833 [M-H$^+$] (99). IR: 3317 (br), 3003 (w), 2955 (w), 2832 (w), 1456 (w), 1381 (w), 1330 (s), 12118 (s), 1109 (s), 1041 (m), 1021 (m), 991 (m), 869 (m), 827 (m), 809 (m), 736 (m), 664 (m), 627 (m) [cm^{-1}]. Elemental analysis calcd. (%) for $C_{19}H_{10}F_{28}O_4$ (834.27): C 27.35 %, H 1.21 %; found: C 27.33 %, H 1.18 %.

X-ray structural data of **5c** (CCDC 827660): $C_{19}H_{10}F_{28}O_4$, formula weight 834.27, crystal size 0.20 x 0.20 x 0.03 mm, crystal system triclinic, space group P1, unit cell dimensions *a* = 10.5910 (7) Å, *b* = 11.4087 (10) Å, *c* = 12.7478 (10) Å, α = 107.199° (4), β = 110.878° (4), γ = 95.198° (4), *Z* = 2, *D*calcd. 2.066 gcm^{-3}, absorption coefficient 0.268 mm^{-1}, wavelength 0.71073 Å, *T* = 100 (2) K, $2\theta_{max}$ = 27.00°, reflections collected/unique 7190/5664 [*R*(int) = 0.0274], final *R* indices [$I > 2\sigma(I)$] *R* = 0.0542, *wR* = 0.1222, largest diff. peak and hole 1.145 and -0.451 eÅ^{-3}.

(4R,5R)-2,2-Dimethyl-4,5-[bis-(diperfluoro-*n*-butyl-hydroxymethyl)]-1,3-dioxolane (5d). Nonafluoro-*n*-butyliodide was used, colorless crystals (592 mg, 26 %) of the product **5d** were obtained by crystallization from *n*-pentane; m.p. 126-129 °C; $[\alpha]_D^{20}$ +2.0 (*c* 0.99, $CHCl_3$). ^{1}H NMR (300.1 MHz, CD_3OD): δ 5.01 (s; 2H), 1.48 (s; 6H). ^{13}C NMR (75.5 MHz, CD_3OD): δ 117.5, 117.4, 117.2, 112.4, 114.7, 111.6, 111.1, 109.1, 108.8, 81.1, 77.1, 25.2. ^{19}F NMR: (282.4 MHz, CD_3OD): δ -82.32 (dd; $^{4}J_{FF}$ 10.5 = Hz, $^{4}J_{FF}$ = 10.5 Hz, $^{3}J_{FF}$ = 2.8 Hz, $^{3}J_{FF}$ = 2.8

Hz, 6F, F-4_B"), -82.39 (dd; $^4J_{FF}$ = 10.2 Hz, $^4J_{FF}$ = 10.2 Hz, $^3J_{FF}$ = 2.8 Hz, $^3J_{FF}$ = 2.8 Hz, 6F, F-4_A"), -109.77 (m; $^2J_{FF}$ = 298 Hz, 2F, F-1_B"); -110.75 (m; $^2J_{FF}$ = 298 Hz, 2F, F-$1_{\underline{B}}$"), -112.93 (m; $^2J_{FF}$ = 297 Hz, 2F, F-1_A"), -114.27 (m; $^2J_{FF}$ = 297 Hz, 2F, F-$1_{\underline{A}}$"), -119.00 (m; $^4J_{FF}$ = 10.5 Hz, 4F, F-2_B", F-$2_{\underline{B}}$"), -120.73 (m; $^2J_{FF}$ = 295 Hz, 2F, F-2_A"), -121.58 (m; $^2J_{FF}$ 295 = Hz, 2F, F-$2_{\underline{A}}$"), -126.8 (m; 4F, F-3_A", F-$3_{\underline{A}}$"), -126.9 (m; 4F, F-3_B", F-$3_{\underline{B}}$"). GCMS: τ_R = 11.11 min; 521, 499, 473, 459, 380, 347, 319, 301, 291, 271, 251, 241, 219, 209, 181, 169, 131, 119, 119, 100, 85, 69, 59; Macherey Optima-5MS; 35 °C, 5 min, 20 °C/min → 280 °C, 10 min; ESI-MS (neg.): m/z (%) = 1033 [M-H$^+$] (99). IR: $\tilde{\upsilon}$ 3341 (br), 2995 (w), 1460 (w), 1391(w), 1350 (m), 1285 (w), 1202 (s), 1132 (s), 1088 (m), 1057 (m), 812 (m), 783 (m), 716 (s) [cm^{-1}]. Elemental analysis calcd. (%) for $C_{23}H_{10}F_{36}O_4$ (1034.31): C 26.71 %, H 0.97 %; found: 26.98 %, H 0.91 %.

X-ray structural data of **5d** (CCDC 827661): $C_{23}H_{10}F_{36}O_4$, formula weight 1034.31, crystal size 0.20 x 0.20 x 0.10 mm, crystal system triclinic, space group P1, unit cell dimensions *a* = 10.8442 (9), *b* = 12.6035 (9) Å, *c* = 13.4532 (6) Å, *α* = 107.292° (4) Å, *β* = 107.556° (6), γ = 97.246° (3), *Z* = 1, *D*calcd. 2.112 gcm^{-3}, absorption coefficient 0.277 mm^{-1}, wavelength 0.71073 Å, *T* = 100(2) K, $2\theta_{max}$ = 27.00°, reflections collected/unique 9338/6861 [*R*(int) = 0.0000], final *R* indices [$I > 2\sigma(I)$] *R* = 0.0752, *wR* = 0.1939, largest diff. peak and hole 1.8864 and -0.903 eÅ^{-3}.

(4R,5R)-2,2-Dimethyl-4,5-[bis-(diperfluoro-*n*-hexyl-hydroxymethyl)]-1,3-dioxolane (5e). Tridecafluoro-*n*-hexyliodide was used, colorless crystals (473 mg, 15 %) of the product **5e** were obtained by sublimation (10^{-2} mbar, 50 °C) or crystallization from *n*-pentane; m.p. 78-79 °C; $[\alpha]_D^{20}$ +1.1 (*c* 0.98, $CHCl_3$). ^{1}H NMR (300.1 MHz, CD_3OD): δ 5.0 (s; 2H), 1.2 (t; 6H). ^{13}C

NMR (100.6 MHz, $CDCl_3$): δ 117.5, 117.1, 115.7, 115.4, 112.4, 111.6, 111.3, 111.05, 110.3, 108.3, 81.3, 77.1, 25.4. ^{19}F NMR: (376.5 MHz, $CDCl_3$): δ -82.38 (m; 6F, F-6_B''), -82.41 (m; 6F, F-6_A''), -109.45 (m; $^2J_{FF}$ = 290 Hz, 2F, F-1_B''), -110.65 (m; $^2J_{FF}$ = 290 Hz, 2F, F-$1_{\underline{B}}$''), -112.62 (m; $^2J_{FF}$ 298 = Hz, 2F, F-1_A''), -113.97 (m; $^2J_{FF}$ = 298 Hz, 2F, F-$1_{\underline{A}}$''), -117.9 (m, 4F, F-2_B'', F-$2_{\underline{B}}$''), -119.5 (m; $^2J_{FF}$ = 295 Hz, 2F, F-2_A''), -121.02 (m; $^2J_{FF}$ = 295 Hz, 2F, F-$2_{\underline{A}}$''), -122.4 (m; 4F, F-3_A'', F-$3_{\underline{A}}$'', F-3_B'', F-$3_{\underline{B}}$''), -123.5 (m; 8F, F-4_A'', F-$4_{\underline{A}}$'', F-4_B'',F-$4_{\underline{B}}$''), -127.3 (m; 8F, F-5_A'', F-$5_{\underline{A}}$'', F-5_B'', F-$5_{\underline{B}}$''). GCMS: τ_R = 13.29 min; m/z = 533, 463, 419, 403, 371, 343, 319, 281, 243, 231, 219, 193, 181, 169, 143, 131, 119, 100, 85, 69, 59, 51; Macherey Optima-5MS; 35 °C, 5 min, 20 °C/min → 280 °C, 10 min. ESI-MS (neg.): m/z (%) = 1433 [M−H$^+$] (99). IR: ν 3337 (br), 2995 (w), 1391 (w), 1362 (w), 1194 (s), 1180 (s), 1086 (m), 1074 (m), 972 (w), 878 (w), 808 (w), 650 (s) [cm^{-1}]. Elemental analysis calcd. (%) for ($C_{31}H_{10}F_{52}O_4$)•H_2O (1462.40): C 25.64 %, H 0.83 %; found: C 25.58 %, H 0.83 %.

X-ray structural data of **5e** (CCDC 827662): $C_{31}H_{10}F_{52}O_4$, formula weight 1034.39 , crystal size 0.30 x 0.10 x 0.05 mm, crystal system triclinic, space group P1, unit cell dimensions *a* = 13.6774 (8) Å, *b* = 13.8975 (10) Å, *c* = 14.0556 (8) Å, *α* = 67.935° (4), *β* = 67.245° (6), *γ* = 83.498° (3), *Z* = 2, *D*calcd. 2.088 gcm^{-3}, absorption coefficient 0.278 mm^{-1}, wavelength 0.71073 Å, *T* = 100 (2) K, $2\theta_{max}$ = 27.00°, reflections collected/unique 11762/9647 [*R*(int) = 0.0191], final *R* indices [$I > 2\sigma(I)$] *R* = 0.0517, *wR* = 0.1160, largest diff. peak and hole 0.949 and -0.680 eÅ^{-3}.

(4R,5R)-2,2-Dimethyl-4,5-[bis-(dipentafluorophenyl-hydroxymethyl)]-1,3-dioxolane (5f). Pentafluorobromobenzene was used, colorless crystals (1.27 g, 70 %) of the product **5f** were obtained by crystallization from petroleum ether; m.p. 130-132 °C; $[\alpha]_D^{20}$ +42.6 (*c* 0.98,

$CHCl_3$), ^{1}H NMR (300.1 MHz, $CDCl_3$): δ 5.41 (s; 2H), 3.98 (s; 2H, OH), 1.40 (s; 6H). ^{13}C NMR (75.5 MHz, $CDCl_3$): δ 145.0, 144.6, 141.1, 141.2, 137.7, 137.8, 117.1, 113.9, 81.6, 78.7, 27.7. ^{19}F NMR (282.4 MHz, $CDCl_3$): δ -132.98 (d; $^3J_{FF}$ = 20 Hz, 4F, F-2_A", F-6_A"), -136.19 (d; $^3J_{FF}$ = 20 Hz, 4F, F-2_B", F-6_B"), -153.43 (tt; $^3J_{FF}$ = 19 Hz, $^4J_{FF}$ = 3 Hz, 2F, F-4_A"), -153.64 (tt; $^3J_{FF}$ = 19 Hz, $^4J_{FF}$ = 3 Hz, 2F, F-4_B"), -161.14 (ddd; $^3J_{FF}$ = 20 Hz, $^3J_{FF}$ = 19 Hz, $^4J_{FF}$ = 5.5 Hz, 4F, F-3_A", F-5_A"), -161.70 (ddd; $^3J_{FF}$ = 20 Hz, $^3J_{FF}$ = 19 Hz, $^4J_{FF}$ = 5.5 Hz, 4F, F-3_B", F-5_B"). GCMS: T_R = 13.17 min; m/z = 463, 385, 363, 295, 195, 181, 167, 101, 59; HP-5MS, 40 °C, 5 min, 5 °C/min → 110 °C, 20 °C/min → 280 °C, 5 min. ESI-MS (neg.): m/z (%) = 825 [M-H$^+$] (60). IR: ν̃ 3390 (br), 2987 (w), 1650 (s), 1523 (s), 1488 (s), 1403 (m), 1372 (m), 1304 (m), 1234 (m), 1117 (m), 1002 (m), 968 (all br), 853 (m), 782 (m), 743 (m), 708 (m) [cm^{-1}]. Elemental analysis calcd. (%) for $C_{31}H_{10}F_{20}O_4$ (826.38): C 45.06 %, H 1.22 %; found: C 45.16 %, H 1.23 %.

X-ray structural data of **5f** (CCDC 798770): $C_{31}H_{10}F_{20}O_4$, formula weight 826.39, crystal size 0.30 x 0.20 x 0.03 mm, crystal system orthorhombic, space group $P22_12_1$, unit cell dimensions *a* = 7.5263 (6), *b* = 11.7755 (10) Å, *c* = 35.090 (3) Å, *Z* = 4, *D*calcd. 1.765 gcm^{-3}, absorption coefficient 0.196 mm^{-1}, wavelength 0.71073 Å, *T* = 100(2) K, $2\theta_{max}$ = 27.00°, reflections collected/unique 9409/3785 [*R*(int) = 0.0523], final *R* indices [$I > 2\sigma(I)$] *R* = 0.0365, *wR* = 0.0627, largest diff. peak and hole 0.327 and -0.264 eÅ^{-3}.

4.5 Crystallization of the 2:1 5a-water complex. This hemihydrate was obtained when the TEFDDOL **5a** was crystallized from non-dried DCM.

X-ray structural data of the 2:1 **5a**-water complex (CCDC 827663): $2(C_{11}H_{10}F_{12}O_4)•H_2O$, formula weight 886.40, crystal size 0.20 x 0.20 x 0.03 mm, crystal

system monoclinic, space group $P2_1$, unit cell dimensions *a* = 15.6960 (7), *b* = 12.2229 (4) Å, *c* =17.2068 (5) Å, *β* = 105.3780 (10)°, *Z* = 4, *D*calcd. 1.850 gcm^{-3}, absorption coefficient 0.226 mm^{-1}, wavelength 0.71073 Å, *T* = 100 (2) K, $2\theta_{max}$ = 27.00°, reflections collected/unique 20898/7274 [*R*(int) = 0.0331], final *R* indices [*I* >2σ(*I*)] *R* = 0.0312, *wR* = 0.0649, largest diff. peak and hole 0.447 and -0.337 eÅ^{-3}.

4.6 Crystallization of the 2:1 5b-water complex. This hemihydrate was obtained when the TEFDDOL **5b** was crystallized from non-dried DCM.

X-ray structural data of the 2:1 **5b**-water complex (CCDC 827659): $2(C_{15}H_{10}F_{20}O_4)\bullet H_2O$, formula weight 1286.48, crystal size 0.30 x 0.20 x 0.10 mm, crystal system monoclinic, space group $P2_1$, unit cell dimensions *a* = 8.1163 (4), *b* = 21.2609 (10) Å, *c* = 12.7665 (3) Å, *β* = 102.562 (3)°, *Z* = 2, *D*calcd. 1.987 gcm^{-3}, absorption coefficient 0.252 mm^{-1}, wavelength 0.71073 Å, *T* = 100(2) K, $2\theta_{max}$ = 27.00°, reflections collected/unique 11214/4791 [*R*(int) = 0.0320], final *R* indices [*I* >2σ(*I*)] *R* = 0.0305, *wR* = 0.0484, largest diff. peak and hole 0.263 and -0.222 eÅ^{-3}.

4.7 Crystallization of the 2:1 5b-DABCO complex. This complex was obtained when a 1:1-mixture of TEFDDOL **5b** and DABCO was crystallized from dry DCM.

X-ray structural data of the 2:1 **5b**-DABCO complex (CCDC 827658): $2(C_{15}H_{10}F_{20}O_4)\bullet C_6H_{12}N_2$, formula weight 1380.64, crystal size 0.15 x 0.10 x 0.03 mm, crystal system orthorhombic, space group $P2_12_12_1$, unit cell dimensions *a* = 10.2080 (6), *b* = 15.1118 (10) Å, *c* = 32.159 (2) Å, *Z* = 4, *D*calcd. 1.849 gcm^{-3}, absorption coefficient 0.225 mm^{-1}, wavelength 0.71073 Å, *T* = 100 (2) K, $2\theta_{max}$ = 27.00°, reflections collected/unique

19818/6004 [*R*(int) = 0.0815], final *R* indices [*I* >2σ(*I*)] *R* = 0.0611, *wR* = 0.1612, largest diff. peak and hole 1.048 and -0.602 eÅ^{-3}.

4.8 Crystallization of the 2:3 5f-DABCO complex. This complex was obtained when a 1:1-mixture of TEFDDOL **5f** and DABCO was crystallized from dry DCM.

X-ray structural data of the 2:3 **5f**-DABCO complex (CCDC 827656): $2(C_{31}H_{10}F_{20}O_4)\bullet3(C_6H_{12}N_2)$, formula weight 1989.31, crystal size 0.30 x 0.20 x 0.10 mm, crystal system monoclinic, space group $P2_1$, unit cell dimensions *a* = 11.0460 (2) Å , *b* = 19.7743 (3) Å, *c* = 18.3995 (3) Å, *β* = 91.3656 (7)°, *Z* = 2, *D*calcd. 1.644 gcm^{-3}, absorption coefficient 0.169 mm^{-1}, wavelength 0.71073 Å, *T* = 100 (2) K, $2\theta_{max}$ = 27.00°, reflections collected/unique 9028/7567 [*R*(int) = 0.0386], final *R* indices [*I* >2σ(*I*)] *R* = 0.0394, *wR* = 0.1038, largest diff. peak and hole 0.755 and -0.464eÅ^{-3}.

4.9 Crystallization of the 1:2 5f-piperidine complex. This complex was obtained when the TEFDDOL **5f** was crystallized from dry DCM in the presence of excess piperidine.

X-ray structural data of the 1:2 **5f**-piperidine complex (CCDC 827657): $(C_{31}H_{10}F_{20}O_4)\bullet2(C_5H_{11}N)$, formula weight 996.69, crystal size 0.40 x 0.20 x 0.10 mm, crystal system orthorhombic, space group $P2_12_12_1$, unit cell dimensions *a* = 10.3791 (4) Å , *b* = 19.8080 (16) Å, *c* = 20.2096 (15) Å, *Z* = 4, *D*calcd. 1.593 gcm^{-3}, absorption coefficient 0.163 mm^{-1}, wavelength 0.71073 Å, *T* = 100 (2) K, $2\theta_{max}$ = 27.00°, reflections collected/unique 17925/5046 [*R*(int) = 0.0588], final *R* indices [*I* >2σ(*I*)] *R* = 0.0410, *wR* = 0.0768, largest diff. peak and hole 0.254 and -0.250 eÅ^{-3}.

4.10 Synthesis of (3aR,5R,6S,6aR)-2,2-dimethyl-3a,5-bis(perfluoroethyl)-tetrahydro-furo[2,3-d][1,3]dioxole-5,6-diol (*rac*-11). According to the General Procedure 4.4, 500 mg of the *meso*-anhydride **10** were reacted. Flash chromatography (EtOAc) afforded colorless crystals (640 mg, 54 %) of the product *rac*-**11**, m.p. 118-120 °C. ^{1}H NMR (300.1 MHz, $CDCl_3$): δ 4.67 (br s; 1H), 4.63 (br s; 1H), 3.32 (s; 2H, OH), 1.50 (s; 3H), 1.37 (s; 3H). ^{13}C NMR (75.5 MHz, $CDCl_3$): δ 120.3-120.6, 119.5, 112.8, 108.9, 79.2, 74.3, 25.3, 23.7. ^{19}F NMR (282.4 MHz, $CDCl_3$): δ -79.81 (d; 3F, $^{3}J_{FF}$ = 14.0 Hz), -79.22 (dd; 3F, $^{3}J_{FF}$ = 14.4, 6.4 Hz), -114.63--119.05 (m; 4F). GCMS: T_R = 9.81 min; m/z = 380, 379, 347, 315, 289, 267, 247, 219, 201, 185, 171, 145, 133, 119, 100 ,85, 69, 59; Macherey Optima-5MS; 35 °C, 5 min, 20 °C/min → 280 °C, 10 min. ESI-MS (neg.): m/z (%) = 411 [M-H$^+$] (99). IR: $\tilde{\nu}$ 3676 (w), 3402 (br), 2988 (w), 2901 (w), 1624 (w), 1451 (w), 1383 (w), 1329 (w), 1177 (m), 1076 (m), 974 (w), 878 (w), 802 (w), 727 (w) [cm^{-1}]. HRMS (ESI-): calcd. for $C_{11}H_{10}F_{10}O_5$ (anion): 411.02848; found: 411.02860 (error < 1 ppm).

X-ray structural data *rac*-**11** (CCDC 827665): $C_{11}H_{10}F_{10}O_5$, formula weight 412.19, crystal size 0.15 x 0.07 x 0.01 mm, crystal system monoclinic, space group $P2_1/c$, unit cell dimensions a = 5.4658 (2) Å, b = 17.8420 (12) Å, c = 15.3081 (3) Å, β = 104.041° (3), Z = 4, Dcalcd. 1.890 gcm^{-3}, absorption coefficient 0.224 mm^{-1}, wavelength 0.71073 Å, T = 100 (2) K, $2\theta_{max}$ = 27.00°, reflections collected/unique 7359/3140 [R(int) = 0.0354], final R indices [I >2σ(I)] R = 0.0360, wR = 0.0538, largest diff. peak and hole 0.295 and -0.278 eÅ^{-3}.

Acknowledgments

Financial support by the Deutsche Forschungsgemeinschaft DFG (Priority Program 1179, “Organocatalysis") and by the Fonds der Chemischen Industrie is gratefully acknowledged.

Supporting Information. NOESY-spectra and DOSY-data of the TEFDDOLs **5b** and **5f**. This material is available free of charge via the Internet at http://pubs.acs.org. The CCDC numbers stated contain the supplementary crystallographic data for this paper. These data can be obtained free of charge from The Cambridge Crystallographic Data Centre via: www.ccdc.cam.ac.uk/data_request/cif.

References

(1) (a) Pihko, P., Ed. *Hydrogen Bonding in Organic Synthesis,* Wiley-VCH: Weinheim, **2009**. (b) Berkessel, A.; Gröger, H. *Asymmetric Organocatalysis*, Wiley-VCH: Weinheim, **2005**. (c) Dalko, P. I., Ed. *Enantiselective Organocatalysis*, Wiley-VCH: Weinheim, **2007**. (d) List, B.; Yang, J. W. *Science* **2006**, *313*, 1584-1586. (e) Melchiorre, P.; Marigo, M.; Carlone, A.; Bartoli, G. *Angew. Chem. Int. Ed.* **2008**, *47*, 6138-6171.

(2) (a) Kotke, M.; Schreiner, P. R. in Pihko, P., Ed. *Hydrogen Bonding in Organic Synthesis*, Wiley-VCH: Weinheim, **2009**, pp. 141-351. (b) Zhang, Z.; Schreiner, P. R. *Chem. Soc. Rev.* **2009**, *38*, 1187-1198. (c) Connon, S. J. *Synlett* **2009**, *65*, 1219-1234. (d) Takemoto, Y. *Org. Biomol. Chem.* **2005**, *3*, 4299-4306.

(3) Aleman, J.; Parra, A.; Jiang, H.; Jørgensen, K. A. *Chem. Eur. J.* **2011**, *17*, 6890-6899. (b) Amendola, V.; Fabbrizzi, L.; Mosca, L. *Chem. Soc. Rev.* **2010**, *39*, 3889-3915.

(4) (a) Gondi, V. B.; Hagihara, K.; Rawal, V. H. *Chem. Commun*. **2010**, 904-906. (b) Villano, R.; Acocella, M. R.; Massa, A.; Palombi, L.; Scettri, A. *Tetrahedron* **2009**, 65,

5571-5576. (c) Huang, Y.; Unni, A. K.; Thadani, A. N.; Rawal, V. H. *Nature* **2003**, *424*, 146.

(5) (a) Seebach, D.; Beck, A. K.; Heckel, A. *Angew. Chem., Int. Ed*. **2001**, *40*, 92-138. (b) Beck, A. K.; Bastani, B.; Plattner, D. A.; Petter, W.; Seebach, D.; Braunschweiger, H.; Gysi, P.; La Vecchia, L. Chimia **1991**, *45*, 238-244. (c) Berkessel, A.; Etzenbach-Effers, K. in Pihko, P., Ed. *Hydrogen Bonding in Organic Synthesis*, Wiley-VCH: Weinheim, **2009**, pp. 15-42. (d) Berkessel, A.; Etzenbach-Effers, K. *Topics Curr. Chem.* **2010**, *291*, 1-27.

(6) Yamamoto, H.; Futatsugi, K. in Yamamoto, H.; Ed. *Acid Catalysis in Modern Organic Synthesis*, Wiley-VCH: Weinheim, **2008**, pp. 1-34.

(7) (a) Shuklov, I. A.; Dubrovina, N. V.; Börner, A. *Synthesis* **2007**, 2925-2943. (b) Bégué, J.-P.; Bonnet-Delpon, D.; Crousse, B. *Synlett* **2004**, 18-29.

(8) Eberson, L.; Hartshorn, M. P.; Persson, O. *J. Chem. Soc., Perkin Trans. 2* **1995**, 1735-1744.

(9) (a) Berkessel, A. in Bäckvall, J. E.; Ed. *Modern Oxidation Methods,* 2nd ed.; Wiley-VCH: Weinheim, **2010**, pp. 117-145. (b) Legros, J.; Crousse, B.; Bonnet-Delpon, D.; Bégué, J.-P. *Tetrahedron* **2002**, *58*, 3993-3998.

(10) (a) Berkessel, A.; Adrio, J.; Hüttenhain, D.; Neudörfl, J. M., *J. Am. Chem. Soc.* **2006**, *128*, 8421-8424. (b) Berkessel, A.; Adrio, J. J*. Am. Chem. Soc.* **2006**, *128*, 13412-13420.

(11) Christ, P.; Lindsay, A. G.; Vormittag, S. S.; Neudörfl, J.-M.; Berkessel, A.; O'Donoghue, A. C. *Chem. Eur. J.* **2011**, *17*, 8524-8528.

(12) (a) Terada, M. *Curr. Org. Chem.* **2011**, *15*, 2227-2256. (b) Rueping, M.; Nachtsheim, B. J.; Ieawsuwan, W.; Atodiresei, I. *Angew. Chem. Int. Ed.* **2011**, *50*, 6706-6720. (c) Yamamoto, H.; Cheon, C. H. in Ojima, I.; Ed. *Catalytic Asymmetric Synthesis*, 3rd ed.; Wiley: Hoboken, **2010**, pp. 119-161. (d) Kampen, D.; Reisinger, C. M.; List, B. *Top. Curr. Chem.* **2010**, *291*, 395-456. (e) Akiyama, T.; Itoh, J.; Fuchibe, K. *Adv. Synth. Catal*. **2006**, *348*, 999-1010.

(13) Burton, D. J.; Yang, Z.-Y. *Tetrahedron* **1992**, *48*, 189-275.

(14) (a) Ruppert, I.; Schlich, K.; Volbach, W. *Tetrahedron Lett.* **1984**, *25*, 2195-2198. (b) Surya Prakash, G. K.; Yudin, A. K. *Chem. Rev*. **1997**, *97*, 757-786.

(15) Hafner, A.; Duthaler, R.; Marti, R.; Rihs, G.; Rothe-Streit, P.; Schwarzenbach, F. *J. Am. Chem. Soc.* **1992**, *114*, 2321-2336.

(16) El Sheikh, S.; Schmalz, H.-G. *Drug Disc. Devel.* **2004**, *7*, 882-895.

(17) Delaney, E. J.; Massil, S. E.; Shi, G.-Y.; Klotz, I. M. *Arch Biochem. Biophys.* **1984**, *228*, 627-638.

(18) Babadzhanova, L. A.; Kirij, N. V.; Yagupolskii, Y. L.; Tyrra, W.; Naumann, D. *Tetrahedron* **2005**, *61*, 1813-1819.

(19) Takemura, H.; Kaneko, M.; Sako, K.; Iwanaga, T. *New. J. Chem.* **2009**, *33*, 2004-2006.

(20) (a) Irurre, J.; Alonso-Alija, C.; Piniella, J. F.; Alvarez-Larena, A. *Tetrahedron: Asymmetry* **1992**, *3*, 1591-1596. (b) Gerard, B.; Sangji, S.; O'Leary, D. J.; Porco, J. A., jr. *J. Am. Chem. Soc.* **2006**, *128*, 7754-7755.

(20) (a) Suhm, M. A., *Adv. Chem. Phys.* **2009**, *142*, 1-57. (b) Schaal, H.; Häber, T.; Suhm, M. A., *J. Phys. Chem. A* **2000**, *104*, 265-274.

(21) Dunitz, J. D.; Taylor, R. *Chem. Eur. J.* **1997**, *3*, 89-98.

(22) Schneider, H.-J. *Chem. Sci.* **2012**, *3*, 1381-1394.

(23) Benoit, R. L.; Lefebvre, D.; Fréchette, M. *Can. J. Chem*. **1987**, *65*, 996-1001.

(24) Crampton, M. R.; Robotham, I. A. J. *Chem. Res*. **1997**, 22-23.

(25) Cabrita, E. J.; Berger, S. *Magn. Reson. Chem.* **2001**, *39*, S142-S148.

(26) Armarego, A. L. F.; Chai, C. L. L. *Purification of Laboratory Chemicals*, 5th ed.; Butterworth-Heinemann: London, **2003**.

(27) Bauer, W. *Magn. Reson. Chem.* **1996**, *34*, 532-537.

(28) Martin, J. S.; Quirt, A. R. *J. Magn. Reson.* **1971**, *5*, 318-327 (modified by R. Sebastian).